UNIVERSITÀ DEL PIEMONTE ORIENTALE

Department of Health Sciences

PhD course in Medical Sciences and Biotechnology

XXXVII cycle

PhD thesis on

Diagnostic Accuracy of PD-L1 Immunohistochemistry Evaluation in Triple Negative Breast Cancer Biopsy

Supervisor:

Prof. Renzo Luciano Boldorini

Candidate:

Dott. Lorenzo Giacometti

Academic year 2025-2026

UNIVERSITÀ DEL PIEMONTE ORIENTALE

Al Coordinatore del Corso di Dottorato
(da inviare insieme alla tesi di dottorato)

DICHIARAZIONE E AUTORIZZAZIONE AL RILEVAMENTO ANTIPLAGIO

(Art. 47 e Art. 38 del D.P.R. 28 dicembre 2000, n. 445) e s.m.i.
esente da bollo ai sensi dell'art. 37 D.P.R. 445/2000 e s.m.i.

Il/La sottoscritto/a Lorenzo Giacometti nato/a a Novara prov (NO) il 1/1/1996, regolarmente iscritto/a per l'a.a. 2025/2026 al 4 anno del Corso di Dottorato di ricerca Scienze e Biotecnologie Mediche, 37 Ciclo

consapevole del fatto che l'Università ha adottato un servizio *web-based* per rilevare il plagio, attraverso un sistema software chiamato "Turnit.in",

consapevole delle sanzioni penali previste in caso di dichiarazioni non veritiere e di falsità negli atti e della conseguente decadenza dei benefici di cui agli artt. 75 e 76 del D.P.R. 445/2000 e s.m.i.,

DICHIARA

- di aver sottoposto la propria tesi di dottorato alla scansione di Turnit.in.

Ritiene che, dalla verifica, la Tesi è ragionevolmente risultata un documento originale, che cita correttamente la letteratura.
È infine consapevole che la propria tesi di dottorato può essere verificata dal proprio Supervisore e/o dal Coordinatore del Corso di dottorato per confermarne l'originalità.

Torino, 15/01/2026 .....
(luogo e data)

.....
(firma)

ABSTRACT

Background: Programmed Death-Ligand 1 (PD-L1) evaluation is essential for predicting response to immune checkpoint inhibitors in advanced Triple-Negative Breast Cancer (TNBC) and determining eligibility for immunotherapy. However, spatial intratumoral heterogeneity raises concerns regarding the representativeness of PD-L1 assessment performed on core needle biopsies (CNBs), potentially leading to the exclusion of eligible patients from effective treatments.

Methods: We compared the concordance of PD-L1 expression between CNBs and matched surgical specimens in a TNBC cohort. Immunohistochemical (IHC) evaluations were conducted using the SP142 clone evaluated with the immune cell (IC) score (the atezolizumab eligibility test) and the E1L3N clone, as a surrogate of the 22C3 clone, evaluated with the combined positive score (CPS) (the pembrolizumab eligibility test). Additionally, we developed two novel selection methods to identify the optimal IHC protocol for E1L3N staining.

Results: The analysis confirmed that PD-L1 expression is frequently underestimated on CNBs compared to surgical specimens. Agreement was "fair" ($\kappa = 0.371$) for the SP142 clone (IC score) and "substantial" ($\kappa = 0.610$) for the E1L3N clone (CPS). Notably, applying the IC score to the E1L3N clone on biopsy specimens yielded a high Negative Predictive Value (NPV) of 93.3% for predicting SP142/IC status, and an NPV of 100% for predicting E1L3N/CPS status.

Conclusions: PD-L1 assessment limited to CNB presents significant challenges in TNBC, particularly with the SP142 assay, due to a high rate of false-negative results that may preclude access to immunotherapy. Our findings suggest that the E1L3N clone (assessed via IC score) could serve as an effective "rule-out" screening test on biopsy material. However, in cases of negative biopsy results, we suggest testing all available archival TNBC tissue and considering a re-biopsy of the primary and metastatic tumor to ensure appropriate therapeutic stratification.

SUMMARY

1 INTRODUCTION

According to the latest WHO report, excluding skin carcinomas, breast carcinoma is the most diagnosed cancer in females and the leading cause of female cancer death worldwide. According to the latest AIOM-AIRTUM report, the Italian prevalence of breast cancer is 925,000 women, of which 37,000 have metastatic neoplasia. The overall 5-year survival rate is 88%[1–3].

1.1 BREAST CANCER BIOLOGICAL SUBTYPES

Breast cancer presents molecular heterogeneity, with different expressions of gene patterns leading to different behavior and prognosis. In recent years, significant efforts have been made to characterize and classify breast cancer at the molecular level, and the analysis of global gene expression patterns has resulted in breast cancer subtypes that are both biologically and clinically significant. However, due to time and costs, a surrogate molecular breast cancer classification was developed, classifying tumors into five subtypes (Table 1) based on the immunohistochemical assessment of the following biomarkers: Estrogen Receptor (ER), Progesterone Receptor (PR), Human Epidermal Growth Factor Receptor 2 (HER2), and Ki-67[3]. Luminal forms of breast cancer constitute about 70% of carcinomas, HER2-positive forms 10-20%, and triple-negative forms 10-15%. There is notable variability in median overall survival (OS) for advanced-stage disease, reflecting the biological behavior of each subtype, as well as treatment effectiveness. French registry data indicate a median OS of 42.9 months for patients with HR-positive/HER2-negative disease, 50.1 months for patients with HER2+ disease, and 14.5 months for triple-negative breast cancer (TNBC). Therapeutic progress over the last decade has significantly increased the median survival for patients with HER2-positive tumors (from 39.1 months in 2008 to 58 months in 2013), but less notably in TNBC (from 14 months in 2008 to 15.1 months in 2013)[2].

Table 1. *"The clinicopathological surrogate definitions of early invasive breast carcinoma subtypes adopted by the 13th St. Gallen International Breast Cancer Conference (2013) Expert Panel, based on immunohistochemical measurements of ER, PR, ERBB2 (HER2), and Ki-67 (proliferation index) with in situ hybridization confirmation where appropriate"*[3].

Breast cancer subtype	Biomarkers status
Luminal A-like	ER: positive
	PR: positive
	HER2: negative
	Ki-67: low
Luminal B-like (HER2-negative)	ER: positive
	HER2: negative
	At least one of the following: • Ki-67: high • PR: negative or low
Luminal B-like (HER2-positive)	ER: positive
	HER2: overexpressed or amplified
	Ki-67: any
	PR: any
HER2-positive (non-luminal)	HER2: overexpressed or amplified
	ER: absent
	PR: absent
Triple-negative	ER: absent
	PR: absent
	HER2: negative

1.1.1 Prognostic and predictive factors assessment in breast carcinoma

1.1.1.1 Hormone receptors evaluation in breast carcinomas

Hormone receptors (HR) expression assessment in breast cancer tissue primarily involves the evaluation of the nuclear expression of ER and PR[3]. The ER nuclear expression evaluation in breast carcinomas is important both for predictive purposes for endocrine therapy and also for pathology classification as ER-positive or ER-negative[3]. The PR nuclear expression tends to be more variable than ER expression and helps to stratify ER-positive cases into prognostic categories, although thresholds for this purpose have not yet been validated. The American Society of Clinical Oncology (ASCO) / College of American Pathologists (CAP) recommends that an IHC expression of ER and PR in at least 1% of tumor cells, with at least weak intensity, be considered positive in breast carcinomas. Additionally, ER positivity between 1% and 10% should be reported as low expression (ER-Low) because, although limited data support the effectiveness of endocrine therapy in this category, the available information suggests a possible therapeutic benefit. Therefore, these patients are eligible for endocrine treatment. This group is also more heterogeneous and biologically behaves more similarly to ER-negative tumors[3]. Finally, ER-negative and PR-negative cases are labeled as HR-negative.

1.1.1.2 HER2 evaluation in breast carcinoma

ERBB2 (HER2) is a member of the family of growth factor receptors, which includes also EGFR (HER1), ERBB3 (HER3), and ERBB4 (HER4), regulating normal cellular proliferation, development, and survival[3].

HER2 protein is weakly expressed on the membrane surface of normal mammary epithelial cells, but in 10-20% of invasive breast carcinomas, there is an overexpression of this protein due to the amplification of its gene. This overexpression can lead to a more aggressive biological behavior of the neoplasm, with increased tumor proliferation, cellular motility, and angiogenesis[3].

HER2 status evaluation in breast cancer involves a combination of immunohistochemistry (IHC) and in situ hybridization (ISH) techniques. The IHC method uses antibodies to detect HER2 protein on the membrane of tumor cells. The staining intensity and type of membrane positivity are evaluated, and HER2 expression is scored on a scale of 0 to 3+ as indicated in Figure 1[4].

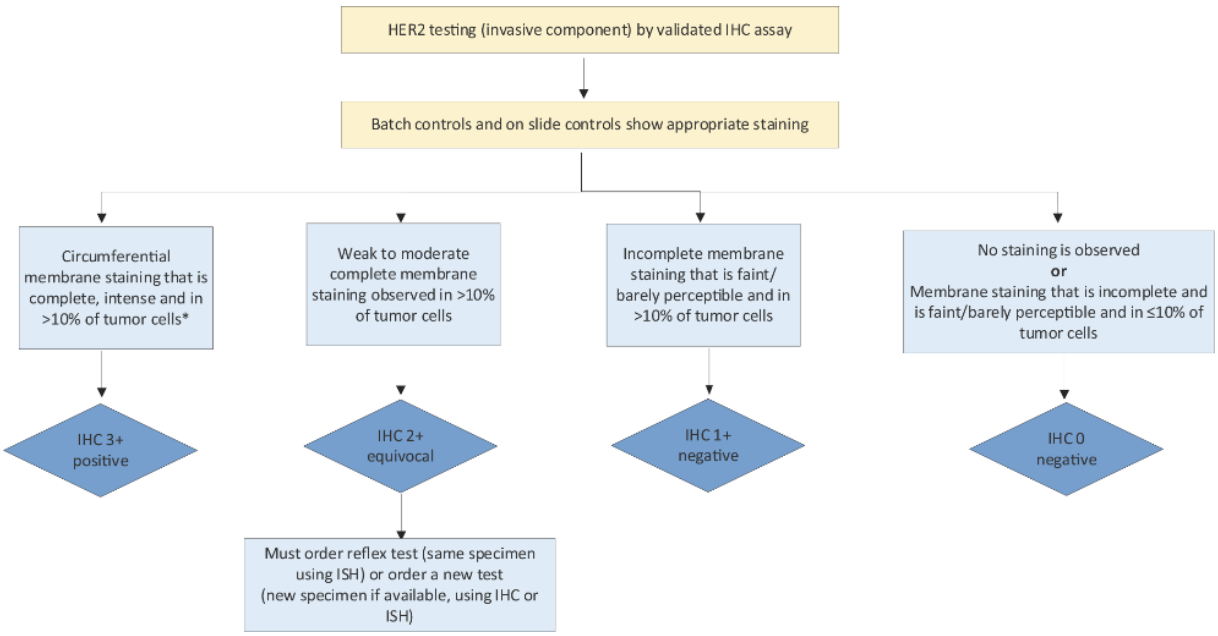

Figure 1. *"The 2018 algorithm for evaluation of human epidermal growth factor receptor 2 (HER2) protein expression by immunohistochemistry (IHC) assay of the invasive component of a breast cancer specimen"*[5].

HER2 IHC scores 0 and 1+ are considered negative for HER2 overexpression, while score 3+ is considered positive. Score 2+ is considered equivocal and requires a confirmatory ISH test that evaluates HER2 gene amplification status using labeled probes that bind specific DNA sequences. The most common ISH method is fluorescence in situ hybridization (FISH), in which fluorescently labeled probes are used to detect the number of HER2 gene copies in tumor cells. The ratio of HER2 gene copies to the number of chromosome 17 (CEP17) copies is used to determine HER2 amplification status[5].

Finally, the combined interpretation of IHC and ISH results determines the HER2 status:

- HER2-positive: IHC 3+ or IHC 2+ with confirmed gene amplification by ISH.
- HER2-negative: IHC 0, IHC 1+, or IHC 2+ without gene amplification.

Currently, several targeted therapies against HER2 are available for HER2-positive breast cancers. The first biologic therapy approved was trastuzumab, an anti-HER2 antibody[3]. Recently, a novel therapy was introduced, named trastuzumab deruxtecan (T-DXd), an antibody-drug conjugate used to treat breast cancer classified as HER2-negative but with low expression of HER2 (IHC 1+ or 2+/ISH non-amplified tumors). Benefits of T-DXd include improved progression-free survival (PFS) and OS compared to standard chemotherapy in patients with HER2-low metastatic breast cancer[6].

1.2 TRIPLE-NEGATIVE BREAST CANCER

TNBC is the term used to describe a category of invasive breast cancer that is HR-negative and HER2-negative. TNBC represents about 15% of new breast cancer diagnoses, including tumors with heterogeneous characteristics and high genomic instability[7]. TNBCs are often characterized by marked aggressiveness and high mortality compared to other breast cancers[8,9].

1.2.1 Triple-negative breast cancer histology

The TNBC group encompasses a wide spectrum of morphologies, grades, and prognosis. However, most TNBCs are high-grade tumors, often presenting with a high nuclear-cytoplasmic ratio, a solid growth pattern, expansive growth margins, geographic necrosis, and typically with a very high mitotic count[3]. The lesions may exhibit a central scar or a large acellular area, and many of them have a dense stromal inflammatory infiltrate. These tumors are rarely associated with an in situ carcinoma component[3]. Tumor-infiltrating lymphocytes (TILs) are defined as mononuclear lymphoid cells that infiltrate the tumor and associated stroma and reflect the host's immune response against the tumor cells. The extent of TILs in invasive breast carcinoma is a prognostic marker associated with a more favorable prognosis and a better response to neoadjuvant therapy in TNBC and HER2-positive cancers[3]. As previously described, TNBC are mostly high-grade tumors but also include low-grade lesions, which can be divided into subgroups: low-grade TNBC (acinic cell carcinoma), breast tumors resembling primitive salivary gland tumors (adenoid cystic carcinoma, secretory carcinoma, adenomyoepithelioma, polymorphous carcinoma, mucoepidermoid carcinoma, and tall cell carcinoma with inverted polarity) and low-grade variants of metaplastic carcinoma (low-grade fibromatosis-like metaplastic carcinoma, and low-grade adenosquamous carcinoma)[10].

1.2.2 Triple-negative breast cancer molecular subclassification

The TNBC group encompasses a heterogeneous group of neoplasms that exhibit various "driver" gene mutations associated with various prognoses. From TNBC gene expression data, four groups have been identified: basal-like 1 and basal-like 2 (which differ in the extent of the associated immune response), mesenchymal, and luminal androgen receptor. These four subtypes exhibit different survival rates and sensitivity to neoadjuvant therapies. Instead, combining RNA and DNA profiling results, TNBCs can also be classified into four subtypes: luminal AR, mesenchymal, basal-like immunosuppressed, and basal-like immune-activated. Each subtype presents specific treatment targets (e.g., androgen receptors and the surface mucin epithelial membrane antigen in the luminal AR subtype) and different prognoses (e.g., the basal-

like immune-activated subtype has a better prognosis than the basal-like immunosuppressed). Despite multiple classification efforts, there is still no established or clinically validated diagnostic test for TNBC classification[3].

1.2.3 Triple-negative breast cancer related immune response

TNBCs are neoplasms characterized by a significant immune response with a high proportion of TILs. Following decades of research in the field of immunology, the key role of T lymphocytes in fighting cancer cells has been emphasized. Nowadays, the use of antibodies capable of blocking immune checkpoints represents a form of immunotherapy with surprising therapeutic effects[11].

1.2.3.1 T lymphocytes activation

The stimulation of the T cell receptor (TCR) by TCR-specific antigens associated with the major histocompatibility complex (MHC) of professional antigen-presenting cells (APCs) leads to the activation and clonal expansion of T lymphocytes. TCR stimulation represents only the initial step. For the activation process, at least a second co-stimulatory signal is required, provided by the interaction between cytotoxic T lymphocyte antigen 4 (CTLA-4) counter-receptor B7.1 (CD80) or CTLA-4 counter-receptor B7.2 (CD86) present on APCs, and the CD28 protein on the surface of T lymphocytes. Lastly, there is also a third signal, mediated by cytokines that induce differentiation and stimulate the effector capabilities of T lymphocytes[12,13].

Other protein interactions modulate the intensity and duration of T lymphocyte activation, such as the interaction between CTLA-4 (CD152) and CD80, making it less available for binding with CD28. Finally, the interaction between programmed death protein-1 (PD-1 / CD279) and programmed death-ligand 1 (PD-L1 / CD274) antagonizes the effect of the second co-stimulatory signal induced by the binding of CD80 and CD28[14].

1.2.3.2 PD-1/PD-L1 Pathway

PD-1 is a transmembrane receptor glycoprotein encoded by the PDCD1 gene, located on chromosome 2[15]. PD-1 protein structure includes three regions: an extracellular immunoglobulin V (IgV) binding domain, a transmembrane region, and an intracellular region characterized by an immunoreceptor tyrosine-based inhibitory motif (ITIM) and an immunoreceptor tyrosine-based switch motif (ITSM)[16]. PD-1 is expressed by immune cells such as T, B, and NK lymphocytes, and its ligands are PD-L1 and programmed death-ligand 2 (PD-L2 / CD273), which are both transmembrane proteins belonging to the B7 family[17]. The PD-L1 protein is widely expressed by a broad spectrum of cell types, including tumor cells, while PD-L2 expression is almost exclusively limited to APCs[17].

PD-L1 protein is encoded by the CD274 gene located on chromosome 9[15]. PD-L1 protein structure has three regions: an extracellular region consisting of two immunoglobulin binding domains, IgV and immunoglobulin C, a transmembrane region, and a cytoplasmic region consisting of a short domain with no known intracellular signaling activity[18].

When PD-L1 interacts with its receptor, phosphorylation of the ITIM and ITSM intracellular domains occurs, allowing for the recruitment of Src homology phosphatase 1 and 2 (SHP-1 and SHP-2)(Figure 2)[19]. SHP-1 and SHP-2 dephosphorylate and thus inactivate the zeta chain of T-cell receptor associated protein kinase 70 (ZAP70) and phosphatidylinositol-4,5-bisphosphate 3-kinase (PI3K) proteins, inhibiting the co-stimulatory signal mediated by the CD28 receptor, which is essential for TCR-mediated signaling (Figure 2)[20,21].

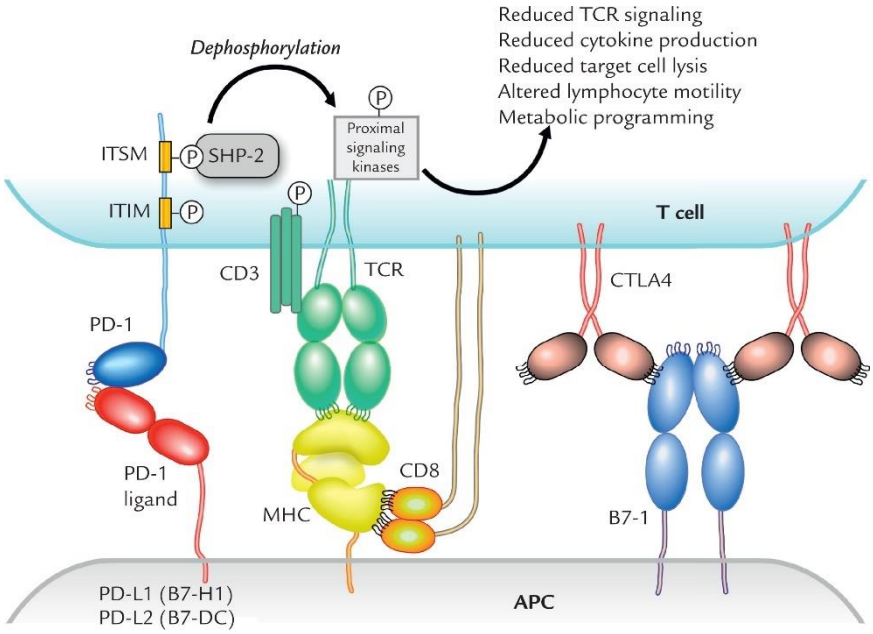

Figure 2. *The interaction between PD-1 and PD-L1 reduces T lymphocyte functionality*[16].

PD-1 receptor also exerts a second-level control on the stimulation induced by CD28 by negatively regulating casein kinase 2 (CK2), which reduces the inhibition of protein phosphatase and tensin homolog (PTEN), thus increasing its activity and counteracting the PI3K-activated signaling pathway[22].

PD-L1 is also present in soluble form (sPD-L1) in the bloodstream, and it is generated by enzymatic cleavage of PD-L1 by extracellular matrix metalloproteases. The sPD-L1 protein retains the IgV domain, necessary for the interaction with the PD-1 receptor. The function of

this soluble ligand is not yet clear, and an increased blood concentration may be associated with a worse prognosis in breast tumors and diffuse large B-cell lymphomas[23].

Therefore, tumor overexpression of PD-L1 can inhibit the immune response associated with the tumor through the PD-1/PD-L1 signaling pathway, making these proteins a therapeutic target for TNBC.

1.2.4 PD-L1 expression evaluation

PD-L1 expression can be present in both tumor cells and inflammatory cells of the tumor microenvironment. Clinically, PD-L1 expression is assessed by a pathologist using IHC. There are different methods to evaluate PD-L1 IHC expression, e.g., immune cell (IC) score, comprehensive positive score (CPS), and tumor positive score (TPS), but only the first two are used for TNBC[9].

1.2.4.1 The immune cell score

The immune cell (IC) score quantifies the proportion of the tumor area occupied by PD-L1-positive immune cells. Only the tumor microenvironment is considered for scoring. The tumor area is defined as the region containing viable tumor cells, including both intratumoral stroma and a contiguous small peritumoral stromal rim. Immune cell types considered in the evaluation include lymphocytes, macrophages, dendritic cells, and stromal-infiltrating granulocytes. All patterns of PD-L1 staining are included, regardless of staining intensity or morphology (e.g., linear, punctate, granular)[9,24,25]. Notably, areas of necrosis, skin ulceration, and granulocytes present within blood vessels and in tissues due to hemorrhagic extravasation are excluded from the tumor area. Only granulocytes actively infiltrating the stromal compartment are included in the count. Finally, PD-L1 expression in tumor cells is not considered in the IC score[26].

IC score is evaluated based on the following formula:

$$IC\ (\%) = \frac{Area\ occupied\ by\ PD-L1\ positive\ immune\ cells}{Tumor\ and\ peritumoral\ stromal\ area} \times 100$$

IC score can be further categorized as follows[25]:

- IC0: <1%
- IC1: ≥1 to <5%
- IC2: ≥5 to <10%
- IC3: ≥10%

1.2.4.2 The combined positive score

The combined positive score (CPS) is used to quantify PD-L1 expression by considering tumor cells and immune cells present intratumorally, and in a narrow rim around the tumor. Tumor cells are considered positive when they show membranous PD-L1 staining, either complete or partial, regardless of intensity. Immune cells include lymphocytes and macrophages exhibiting membranous and/or cytoplasmic staining. The sum of these positive cells is then divided by the number of viable tumor cells in the tumor area and multiplied by 100. Although the calculated value may exceed 100, the maximum score that can be assigned is 100[9,25].

CPS is evaluated based on the following formula:

$$CPS = \frac{Number\ of\ PD-L1\ positive\ cells\ (tumor\ cells,\ lymphocytes,\ macrophages)}{\text{Total number of viable tumor cells}} \times 100$$

1.3 IMMUNOTHERAPY IN BREAST CANCER

Breast cancer, historically considered poorly immunogenic, has become a focus of intense research in the field of immunotherapy. Recent advances in immunobiology and the success of immune checkpoint inhibitors (ICIs) in other malignancies have led to the exploration of various immunotherapeutic strategies for breast cancer[27,28]. ICIs aim to overcome tumor-induced immune suppression and to reactivate the immune system against tumor cells[29].

The actual therapeutic strategy based on immunotherapy for breast cancer relies on ICIs, in particular, on two monoclonal antibodies targeting the PD-1/PD-L1 pathway, atezolizumab and pembrolizumab, which are approved by the European Medicines Agency (EMA) for TNBC[30,31].

1.3.1 Atezolizumab in triple-negative breast cancer

Atezolizumab is a humanized immunoglobulin G1 (IgG1) monoclonal antibody designed to target and bind to PD-L1. By disrupting the PD-1/PD-L1 interaction, atezolizumab reverses T-cell suppression, enabling the immune system to recognize and destroy cancer cells more effectively[32]. Different studies investigated atezolizumab efficacy in TNBC with differences based on the clinical settings and the therapeutic combination used.

In advanced or metastatic TNBC (aTNBC, mTNBC), the IMpassion130 phase III trial demonstrated improved PFS when atezolizumab was combined with nab-paclitaxel as a first-line treatment. While initial results led to accelerated Food and Drug Administration (FDA) approval of atezolizumab combined with nab-paclitaxel, this approval was later withdrawn due to a lack of clinical benefit in the intention-to-treat (ITT) population. Although significant PFS was gained by ITT (7.2 months vs. 5.5 months) and PD-L1-positive subgroup (IC score >1%; 7.5 months vs. 5.0 months), the study did not reach statistical significance in the final OS analysis. The drug benefit was more pronounced in patients with PD-L1-positive tumors, with a median OS of 9.5 months. In this cohort, PD-L1 expression was evaluated on multiple samples from different anatomical sites and across various specimen types (e.g., CNB, excisional, incisional, punch, and forceps biopsies)[32]. These results suggest a clinically meaningful OS benefit with atezolizumab plus nab-paclitaxel in this category of patients. However, this analysis could not be formally performed due to the prespecified statistical testing hierarchy[27].

Another study, IMpassion131, evaluated atezolizumab combined with paclitaxel (instead of nab-paclitaxel) and found no improvement in either PFS or OS, even in the PD-L1-positive subgroup. In this study, the control group reached an OS of 22.8 months, a result without clinical precedent, which likely influenced the study's outcomes. The discrepancy in results between IMpassion130 and IMpassion131 is unclear and could be explained by the use of

immunosuppressive steroids as premedication with paclitaxel, which may have interfered with atezolizumab's effect[27,33].

In the early-stage disease setting, the phase III IMpassion031 trial showed a significant increase in pathological complete response (pCR) rates (58% vs. 41%) when atezolizumab was combined with neoadjuvant chemotherapy, regardless of PD-L1 expression. However, the phase III NeoTRIPaPDL1 trial did not confirm the latter result. Furthermore, the phase III IMpassion132 trial, which evaluated atezolizumab in combination with chemotherapy in early relapsing TNBC, revealed no significant differences in terms of disease-free interval or OS. Such outcomes, aligned with KEYNOTE-355 exploratory analyses on relapses occurring within 12 months, suggest the hypothesis of an intrinsic immunotherapy resistance in specific rapidly relapsing TNBC[27,29].

1.3.2 Pembrolizumab in triple-negative breast cancer

Pembrolizumab is a highly selective, humanized immunoglobulin G4 (IgG4) monoclonal antibody that targets PD-1. It is designed to block the interaction of the receptor with PD-L1 and PD-L2, and it allows the activation of an antitumor response with durable antitumor activity and manageable safety in mTNBC. Several studies have investigated pembrolizumab as a monotherapy in patients with aTNBC or mTNBC, who were treatment-refractory and exhibited PD-L1-positive disease [29,34].

The KEYNOTE-012 phase Ib trial investigated the use of single-agent pembrolizumab in PD-L1-positive (PD-L1 expression in the stroma or in ≥ 1% of tumor cells) aTNBC patients and showed an encouraging overall response rate of 18.5%[35].

The phase II KEYNOTE-086 study found an objective response rate (ORR) of 21.4% when pembrolizumab was used as a first-line treatment for PD-L1-positive mTNBC, and a more modest ORR of 5.3% calculated regardless of PD-L1 expression levels in previously treated mTNBC[36]. These studies indicate the benefit of ICIs therapy in PD-L1-positive TNBC, with greater effect when used early in the treatment course[27].

The phase III KEYNOTE-119 study compared pembrolizumab monotherapy with investigator's choice chemotherapy (capecitabine, gemcitabine, eribulin, or vinorelbine) in previously treated mTNBC patients. Although no differences in PFS or OS were observed, a graded ORR to pembrolizumab was found with higher PD-L1 expression tumors, with the greatest benefit observed in patients with PD-L1 CPS ≥ 10[27,29].

The KEYNOTE-355 study evaluated pembrolizumab as a first-line therapy for aTNBC and mTNBC, administered in conjunction with investigator-choice chemotherapy, including paclitaxel, nab-paclitaxel, or the combination of gemcitabine and carboplatin. The study

showed a significant and clinically meaningful improvement in PFS and led to the drug's approval by the FDA in November 2020 for patients with PD-L1-positive tumors. Recently, a significant benefit in PFS (9.7 months vs. 5.6 months) and OS (23.0 months vs. 16.1 months) was confirmed in patients with PD-L1 CPS ≥10 (assessed by IHC 22C3 pharmDx)[28], based on an analysis of multiple samples per patient across different anatomical sites and specimen types[37].

The phase 3 trial KEYNOTE-522 evaluated early-stage TNBC patients, who received neoadjuvant pembrolizumab or placebo with chemotherapy, and continued pembrolizumab after surgery until a full year of treatment. Pembrolizumab regimen was associated with a pCR rate of 64.8% compared to 51.2% of the placebo group, and with a significantly lower recurrence risk (HR 0.63). Based on this study, in 2021, the FDA granted approval of pembrolizumab for neoadjuvant and adjuvant therapy. The KEYNOTE-522 regimen is the current standard of care for early-stage TNBC[27,38].

1.3.3 Immune checkpoint inhibitor therapy eligibility test

Following a diagnosis of aTNBC on core needle biopsy (CNB), PD-L1 expression is assessed to predict the potential response to ICIs therapy. Currently, in the advanced setting, ICIs are indicated in combination with chemotherapy exclusively for PD-L1-positive TNBC. The companion diagnostic test specific to each study protocol formally determines the eligibility for a particular ICI. Specifically, PD-L1 IC score ≥1% assessed using the Ventana PD-L1 SP142 IHC assay (Roche), qualifies a patient for atezolizumab therapy in Europe only. Instead, PD-L1 CPS ≥10, evaluated using the PD-L1 22C3 IHC assay (Dako Agilent), allows a therapy with pembrolizumab[2].

1.3.4 The use of immune checkpoint inhibitors in non-triple-negative breast cancer

A meta-analysis of nine randomized clinical trials involving 5,114 early-stage breast cancer patients (2,097 TNBC, 1,924 HR-positive/HER2-negative, and 1,115 HER2-positive) assessed the efficacy and safety of adding ICIs to neoadjuvant chemotherapy. The studies evaluated atezolizumab, pembrolizumab, durvalumab, and nivolumab. The addition of ICIs to neoadjuvant chemotherapy improved pCR rates in TNBC regardless of PD-L1 status, and in HR-positive/HER2-negative tumors only in the PD-L1-positive cohort, but no benefit was achieved in HER2-positive tumors. Instead, in the adjuvant setting, ICIs showed no pCR or residual disease improvement. Considering the financial cost and the serious adverse events (AEs) associated with these therapies, future investigations should prioritize the identification

of predictive biomarkers to better select patients who would derive the greatest clinical benefit from the integration of ICIs into neoadjuvant chemotherapy protocols[39].

1.3.5 Safety profile of immune checkpoint inhibitors in triple-negative breast cancer

The combination of ICIs with chemotherapy for TNBC can lead to various AEs. While nab-paclitaxel alone may result in chemotherapy-related AEs, combining atezolizumab with nab-paclitaxel can also lead to immune-related AEs, including hematological, pulmonary, endocrine, and neurological AEs[40].

AEs can be classified as either severe or non-severe. The incidence of serious immune-related AEs correlated with ICIs treatment was low but significantly higher than with chemotherapy alone. Some examples of serious AEs are pneumonitis, hypothyroidism, alanine aminotransferase elevation, and adrenal insufficiency[41]. Moreover, the occurrence of non-serious AEs was also higher in patients treated with ICIs compared to those receiving chemotherapy alone. The most frequently reported AEs included elevated aspartate aminotransferase, hypothyroidism, pruritus, rash, and fever[41]. Pembrolizumab has shown a worse safety profile than atezolizumab, causing more grade ≥ 3 AEs with a significant increase in adrenal insufficiency, diarrhea, and infusion reaction. Therefore, atezolizumab represents a safer therapeutic option in patients eligible for treatment[42].

1.4 TRIPLE-NEGATIVE BREAST CANCER TREATMENT

The oncologic treatment guidelines classify breast cancer based on the disease extension, dividing it between early-stage breast cancer and advanced breast cancer. This distinction is crucial because it guides treatment decisions and provides information about prognosis.

Early-stage breast cancer describes a neoplasia that is confined to the breast and regional lymph nodes without distant metastatic spread. The goal of the treatment at this stage is to cure. The management strategy is based on a multidisciplinary approach, which usually starts with surgery and can include radiation and systemic therapy, but can also be preceded by a neoadjuvant treatment, depending on the individual case[38].

Advanced breast cancer includes both locally advanced inoperable disease (not operable with mastectomy) and metastatic disease that has spread beyond the breast and regional lymph nodes to distant organs. The goal of the treatment at this stage shifts from cure to disease control and symptom relief. The management strategy is complex and individualized, with the use of systemic therapies like chemotherapy, hormone therapy, and targeted therapies, which play a larger role in these settings. Finally, palliative care focuses on relieving symptoms and improving the quality of life[2].

1.4.1 Early-stage triple-negative breast cancer treatment

Treatment for early-stage TNBC typically includes surgery, radiation, and chemotherapy. The administration of systemic therapy in the neoadjuvant setting has been shown to provide OS and distant recurrence rates comparable to the postoperative adjuvant setting. Neoadjuvant therapy offers several important advantages, firstly, tumor downstaging, which may allow for a breast-conserving surgery in cases where it was initially not feasible. Secondly, it provides a prognostic assessment based on the individual pathological response to neoadjuvant systemic treatment. Lastly, it allows a personalization of adjuvant therapy, guided by the presence of residual disease after neoadjuvant treatment. However, neoadjuvant therapy may be associated with a slightly increased risk of local recurrence, which is partly attributed to the more frequent use of breast-conserving surgery and, in some cases, to the omission of surgery altogether[2].

The European Society for Medical Oncology (ESMO) defines neoadjuvant therapy as the standard treatment for cT1c or greater TNBC, except for low-grade TNBC of specific histotypes (e.g., adenoid cystic carcinoma, secretory carcinoma). Neoadjuvant systemic therapy for TNBC is primarily based on chemotherapy regimens, with the addition of pembrolizumab for selected cases, as indicated by the KEYNOTE-522 study. In this setting, pembrolizumab is approved by the EMA and the Italian medicines agency (AIFA), and in Italy is reimbursed by the Italian national health service in combination with chemotherapy, followed by monotherapy adjuvant

treatment after surgery for patients with early-stage TNBC at high risk of recurrence (cT1c cN1–N2; cT2–4 cN0–N2). Importantly, IHC PD-L1 expression does not have a predictive value in neoadjuvant pembrolizumab therapy for TNBC[38,43].

1.4.2 Advanced triple-negative breast cancer treatment

Advanced TNBC treatment requires a multimodal and personalized therapeutic approach based on specific disease characteristics and patient status. According to AIOM and ESMO guidelines, the systemic treatment is guided by molecular stratification, particularly by germline BRCA1/2 mutations assessment and by PD-L1 expression evaluation[2,44].

The first-line treatment for PD-L1-positive TNBC is based on ICI combined with chemotherapy:

- Pembrolizumab with chemotherapy is preferred if the tumor expresses PD-L1 with CPS ≥10.
- Atezolizumab with nab-paclitaxel is approved in Europe by EMA and reimbursed in Italy for tumors that express PD-L1 with an IC score ≥1%. However, this indication is no longer approved by the FDA following the voluntary withdrawal by the manufacturer after reassessment of confirmatory trial data[45].

Patients with metastatic TNBC who are PD-L1 negative and carry pathogenic or likely pathogenic germline BRCA1/2 variants can be treated with PARP inhibitors (olaparib, talazoparib), preferred over chemotherapy. In the absence of predictive biomarkers, chemotherapy remains the standard treatment for aTNBC. Although the combination of bevacizumab and paclitaxel has been shown to improve objective response rate and PFS, it does not confer a significant OS benefit. In Italy, bevacizumab is approved and reimbursed in combination with paclitaxel as a first-line treatment[2].

Other therapeutic options are represented by trastuzumab deruxtecan (T-DXd), which is a potent antibody-drug conjugate (ADC) that targets the HER2 protein. This ADC has shown impressive efficacy in patients with HER2-low tumors. This drug is indicated and reimbursed in Italy for advanced TNBC after at least one line of chemotherapy and is also indicated but not reimbursed for HER2-ultralow tumors (HER2 score 0, with a percentage of neoplastic positive cells greater than 0 but lower than 10%). A useful third-line therapy is based on sacituzumab govitecan, another ADC directed against the surface antigen TROP2, which is indicated by ESMO and AIOM, and is reimbursed in Italy[2,44].

1.5 PD-L1 ANTIBODIES OTHER THAN COMPANION DIAGNOSTICS

For PD-L1 expression assessment in TNBC, antibody clones, IHC platforms, and scoring methods are not fully interchangeable. Specifically, the SP142 assay performed on the Ventana platform and evaluated using the IC score, and the 22C3 assay executed on the Autostainer Link 48 platform (Dako Agilent) and assessed with the CPS, identifies different patient subpopulations. An exception to this statement is represented by the SP263 clone conducted on the Ventana platform. Recent evidence demonstrated that CPS can be reliably and accurately assessed in TNBC using either the 22C3 or the SP263 assay, provided that each assay is performed on its designated staining platform[46].

Several anti-PD-L1 antibody clones were employed in research settings[47]. Among them, the E1L3N clone (Cell Signaling) was widely used and has been cited in over 1,000 scientific publications[48]. This clone has shown high concordance with the Ventana SP263 and Dako 22C3 antibodies for PD-L1 expression assessment using TPS in non-small-cell lung cancer (NSCLC)[49]. Similarly, high concordance has been reported in TNBC between the E1L3N clone and the SP263 clone when evaluated with the IC score[50,51] and between the E1L3N clone and the 22C3 clone using CPS[52]. The E1L3N clone has been clinically validated in NSCLC when paired with the Leica BOND-MAX platform[53]. However, it has not yet been formally validated for PD-L1 expression assessment in TNBC. Moreover, studies employing this antibody have used a variety of platforms, detection systems, and staining protocols, often without fully reporting methodological details[49,54]. Therefore, to use the E1L3N antibody for PD-L1 evaluation in TNBC without the Leica platform, it is necessary to optimize, or even validate, a new IHC protocol on alternative platforms, such as the Ventana BenchMark Ultra.

1.6 HETEROGENEITY OF PD-L1 EXPRESSION IN TRIPLE-NEGATIVE BREAST CANCER

PD-L1 expression can be detected across various breast cancer types, and its expression is notably elevated in TNBC[8,55]. This higher expression is particularly evident in high-grade TNBCs, including ductal carcinomas with medullary features, high-grade metaplastic carcinomas, and carcinomas with neuroendocrine features[55]. PD-L1 expression in TNBC exhibits significant heterogeneity, which poses a challenge for accurate patient stratification for ICI therapies. This heterogeneity can be observed at different levels. Firstly, TNBC shows heterogeneous intratumoral expression of PD-L1, which can vary substantially within the same tumor (e.g., tumor center, tumor/stroma interface)[56]. Studies using tissue microarrays and whole cancer sections have demonstrated that different areas of a tumor may exhibit varying percentages of PD-L1-positive cells[57]. Lastly, TNBC is characterized by PD-L1 heterogeneous expression between neoplastic sites, with primary neoplasms that can demonstrate higher PD-L1 expression than metastatic localizations[55,58].

2 AIM OF THE STUDY

Given the heterogeneity of PD-L1 expression in TNBC, and the observation that extensive positivity (>50%) across the tumor mass is rarely encountered[8,55,56], the primary objective of this study was to compare PD-L1 IHC expression between diagnostic CNBs and corresponding surgical specimens in TNBC patients. This comparison aimed to determine whether biopsy samples reliably reflect the PD-L1 status of the resected tumor. The analysis was conducted using the SP142 clone to evaluate the representativeness of PD-L1 assessment for atezolizumab eligibility, and the E1L3N clone, selected as a surrogate of the 22C3 clone, to evaluate PD-L1 expression for pembrolizumab eligibility.

When suboptimal concordance between PD-L1 assessment in biopsy and surgical specimens was demonstrated, specific measurable biopsy parameters were analyzed to assess if they could affect the representativeness of PD-L1 evaluation.

Finally, the study compared PD-L1 expression results obtained using E1L3N and SP142 clones evaluated with the CPS and IC score, to explore the potential interchangeability between antibodies and scoring methods for PD-L1 IHC assessment.

3 MATERIALS

All materials used in this study are listed by category in the following tables (from Table 2 to Table 6).

Table 2. *Antibodies.*

Clone	Antigen	Host	Catalog ID	Supplier
E1L3N	PD-L1	Rabbit mAb	13684	Cell Signaling Technology
SP142	PD-L1	Rabbit mAb	740-4859	Ventana, Roche

Table 3. *Immunohistochemistry reagents and kits.*

Name	Description	Catalog ID	Supplier
OptiView DAB	IHC detection kit	760-700	Ventana, Roche
OptiView amplification kit	Signal amplification	760-099	Ventana, Roche
UltraView universal DAB	IHC detection kit	760-500	Ventana, Roche
Amplification kit	Signal amplification	760-080	Ventana, Roche
Hematoxylin II	Counterstain	790-2208	Ventana, Roche
Bluing reagent	Post counterstain	760-2037	Ventana, Roche
Antibody diluent	Antibody diluent	251-018	Ventana, Roche

Table 4. *Consumables.*

Name	Description	Catalog ID	Supplier
TOMO adhesion microscope slide	IHC microscope slide	TOM-1190	Matsunami Glass
EZ prep solution (10x)	Paraffine removal solution	950-102	Ventana, Roche
ULTRA LCS	Coverslip solution	650-210	Ventana, Roche
Reaction buffer concentrate (10x)	Buffer	950-300	Ventana, Roche
ULTRA cell conditioning 1	Unmasking solution	950-224	Ventana, Roche

Table 5. Instruments.

Name	Description / Use	Catalog ID	Supplier
Donatello series 3	Tissue processor	SDSDT9000	Diapath
TS 8056	Oven	N.D.	Termaks
HM 335 E	Microtome	8243-30-0001	Microm
DPH 35	Tissue floating bath	53DPH35000	Diapath
VENTANA BenchMark ULTRA IHC/ISH system	IHC slide staining system	N750-BMKU-FS	Ventana, Roche
VENTANA HE 600	Slides coverslipping	06917259001	Ventana, Roche
VENTANA DP 200	Slide scanner	08303916001	Ventana, Roche
Aperio GT 450 DX	Slide scanner	23GT450	Leica Biosystems Imaging, Inc.

Table 6. *Software.*

Name	Description	Version	Supplier
WINSAP	Laboratory information system	3.0	Engineering
Excel	Spreadsheet calculator	2509	Microsoft
QuPath	Software for digital pathology image analysis	0.5.0	Open source / University of Edinburgh
Jamovi	Statistical platform	2.6	Open source / The jamovi project

4 METHODS

4.1 PATIENTS

Patients were selected based on strict inclusion and exclusion criteria as reported in the following list.

Inclusion criteria:

- Age ≥18 years.
- TNBC diagnosis on CNB, confirmed on surgical resection specimen.
- At least 100 viable neoplastic cells of invasive breast cancer in both biopsy and surgical specimen formalin-fixed and paraffin-embedded (FFPE) tissue sections.
- Biopsy performed after 2018-06-01.

Exclusion criteria:

- Diagnosis of non-epithelial neoplasms or cutaneous epithelial carcinomas of the breast area.
- Diagnosis of breast metastases from non-breast primary carcinomas.
- Diagnosis of in situ breast carcinomas without invasive components in any FFPE tissue samples.
- Patients treated with neoadjuvant therapy.

4.1.1 Identification of TNBC patients

To select TNBC patients, data extraction was performed using the laboratory information system of the participating pathology departments. Different textual keywords were searched in the diagnosis field (“HER”, “Her”, “ErbB2”, “Erb-B2” or “erbB2”), confining the search to departments where breast biopsies or surgeries were performed (e.g., radiology, breast surgery, general surgery, gynecology). These keywords were used for identifying patients affected by invasive breast carcinoma, in which prognostic and predictive factors were evaluated. The extracted reports were temporarily collected in a password-protected Excel file and semi-automatically analyzed using three Visual Basic for Applications (VBA) scripts specifically written to analyze HER2, ER, and PR values from each report (Supplementary materials, Visual basic for applications scripts section, from Script 1 to Script 3). The extracted prognostic/predictive factor values were classified using a specific VBA script (Supplementary materials, Visual basic for applications scripts section, Script 4) as TNBC, luminal-like, or HER2-positive (non-luminal). Additionally, the latter script was able to identify cases where ISH report verification was necessary to confirm TNBC (HR-negative / HER2-equivocal).

After ISH reports reviews, histological slides from CNB and surgical specimens were examined using an optical microscope, and a representative FFPE tissue block from the archival tissues of the surgical sample was selected, specifically the one with the most extensive tumor-stroma interface. Finally, patients whose material met all the selection criteria were included in a pre-selection list.

4.1.2 Ethical committee approval of the multicenter study

Considering the low incidence of TNBC and the increasing trend of using neoadjuvant chemotherapy for this neoplasia, it was necessary to design a multicenter prospective and retrospective study.

The following centers participated in the study:

- Azienda Ospedaliero-Universitaria SS. Antonio and Biagio, and Cesare Arrigo of Alessandria.
- Azienda Ospedaliero-Universitaria Maggiore della Carità of Novara.
- Azienda Sanitaria Locale of Verbano Cusio Ossola.
- Azienda Sanitaria Locale of Vercelli.

The study protocol was approved by the intercompany ethics committee of Novara, the competent ethics committee of all the participating institutions.

4.1.3 Patient sample

A total of 49 female patients were enrolled in the study. The only clinical parameter collected was the greatest tumor dimension, as reported in the histopathological evaluation of the surgical resection specimen. No additional clinical data were recorded, as they were judged irrelevant to the specific objectives of the study.

4.2 PD-L1 IMMUNOHISTOCHEMICAL EVALUATION

4.2.1 Antibody selection

An ideal choice for this study would have been to use the antibodies and platforms validated as companion diagnostics for the drugs used in TNBC treatment, specifically the SP142 clone on the Ventana platform and the 22C3 clone on the Dako platform. However, due to the unavailability of the Dako platform, we chose the SP142 clone, donated by Roche, and the E1L3N clone (Cell Signaling), selected as a surrogate of the 22C3 clone, both performed on the Ventana platform. Given the absence of a validated protocol for the E1L3N clone on the Ventana platform for PD-L1 assessment in TNBC, it was necessary to optimize an IHC protocol for this study. To ensure greater objectivity, we also developed two novel methods to select IHC protocols that minimize reliance on subjective interpretation of a pathologist and reduce the necessity of a specialist with extensive experience in IHC protocol optimization.

4.2.2 The SP142 clone immunohistochemical protocol

The SP142 clone is used as part of a clinical in vitro diagnostic (IVD) assay, performed with the OptiView diaminobenzidine (DAB) IHC detection kit and the OptiView amplification kit on the Ventana BenchMark ULTRA platform. The protocol is established by the manufacturer and cannot be modified by the user (Table 7).

Table 7. *SP142 clone IHC protocol for Ventana Benchmark Ultra.*

Characteristics	Details
Detection kit	OptiView
Deparaffinization	Selected
Cell conditioning	ULTRA CC1, 48 minutes
Pre-primary peroxidase inhibition	Selected
Antibody dispensation	Automatic
Primary antibody	Ready to use, 16 minutes at 36°C
OptiView HQ linker	8 minutes
OptiView multimer	8 minutes
Amplification	Selected
H_2O_2 amplification	8 minutes
Multimer amplification	8 minutes
Counterstaining	Hematoxylin II, 8 minutes
Post-counterstaining bluing	Bluing reagent, 4 minutes

4.2.3 E1L3N clone immunohistochemical protocol optimization

Seven different protocols inspired by scientific papers were tested and compared to optimize PD-L1 IHC staining using the E1L3N clone. The primary antibody concentration was maintained constant for all the protocols, as set by Adam et al[49]. The protocols varied in terms of tissue antigen retrieval time, primary antibody incubation time and temperature, detection kit, and the use of signal amplification systems with different incubation times. Detailed descriptions of the protocols can be found in the Supplementary materials (Immunohistochemistry protocols section, from Table 19 to Table 24).

A normal tonsil specimen was used to test the protocols. The tissue was fixed in 10% neutral buffered formalin for 24 hours and processed according to the routine methods of the pathology laboratory of the Azienda Ospedaliero–Universitaria Maggiore della Carità of Novara. Consecutive 4 µm-thick histological sections from the FFPE sample were prepared, and the sections were placed on high-adhesive slides and left to dry at room temperature overnight. The following day, all sections were baked in an oven at 60°C for 30 minutes and stained using the Ventana BenchMark ULTRA system according to the study protocols. A 1:100 dilution of the E1L3N antibody was prepared starting from the original product concentration, and a manual dispensing of 100 µl was performed.

The immunohistochemical staining protocols were evaluated using three different methods:

- Ranking by pathologists, based on overall staining quality and personal preference.
- Optical staining evaluation of predefined tissue areas.
- Semi-automated evaluation of predefined tissue areas.

4.2.3.1 Ranking by pathologists

Two pathologists independently assessed the slides stained, in a blind manner, according to the study protocols using an optical microscope at 200x magnification. Protocols were ranked from best to worst based on the estimation of the ratio between specific signal intensity and background noise (Table 8).

Table 8. *Immunohistochemistry protocols ID rankings by pathologist (final protocol in bold).*

Ranking (No.)	Pathologist No.1	Pathologist No.2
1	205	**212**
2	**212**	210
3	207	205
4	203	211
5	210	203
6	197	197
7	211	207

4.2.3.2 Optical staining evaluation of predefined tissue areas

Two pathologists performed independent assessments of stained slides, in a blind manner, according to the study protocols, using an optical microscope at 200x magnification. Predefined tissue areas were selected for the evaluations. Specifically, two categories of histological structures were chosen. The first one, the positive category, included structures expected to exhibit specific PD-L1 expression (i.e., germinal center, mantle, and crypt epithelium). The second one, the negative category, comprised structures not expected to show specific PD-L1 expression (i.e., superficial epithelium, salivary glands, stroma, red blood cells).

For each IHC slide, the three predefined areas per structure type were assessed, as indicated in the Supplementary materials (Predefined reference areas section, Figure 6 and Figure 7). Positive category structures were evaluated by scoring the intensity of both the expected positive cells (signal) and the background staining (noise) using a scale of values from 0 to 6, based on the predefined reference intensity scale provided in the Supplementary materials (Intensity scale reference section, Figure 8). Negative category structures were scored only as background staining (noise), using the same scale. Areas affected by artifacts (e.g., tissue tears, section folds, pigment deposits) were excluded from the analysis. The scores assigned by the two pathologists were combined by summing them, and the results were recorded in a spreadsheet for data analysis.

For each positive category structure (e.g., germinal center), the staining value was calculated using the formula:

$$= \text{MEAN}(\text{signal\_area\_1}; \text{signal\_area\_2}; \text{signal\_area\_3}) - \text{MEAN}(\text{noise\_area\_1}; \text{noise\_area\_2}; \text{noise\_area\_3})$$

For each negative category structure (e.g., red blood cells), the staining value was calculated using the formula:

$$= \text{MEAN}(\text{noise\_area\_1}; \text{noise\_area\_2}; \text{noise\_area\_3})$$

Subsequently, an overall mean value was calculated for both the positive structures category and the negative structures category. The difference between these two means was then calculated, and based on these results, a protocol ranking was listed (Table 9).

Table 9. *Results from the optical staining evaluation of predefined tissue areas (final protocol in bold).*

	Positive category				Negative category					
Protocols ID	Germinative center	Mantel	Crypt epithelium	Mean of positive category	Superficial epithelium	Salivary glands	Stroma	Red blood cells	Mean of negative category	Difference between means
212	8,67	11,00	5,33	8,33	3,33	4,00	2,33	4,00	3,42	4,92
205	3,00	4,00	6,67	4,56	0,67	1,00	3,67	1,67	1,75	2,81
210	6,67	6,67	3,67	5,67	2,00	7,67	3,00	3,67	4,08	1,58
207	2,33	2,00	5,33	3,22	2,00	0,67	3,33	2,33	2,08	1,14
211	6,33	7,33	5,33	6,33	5,33	8,67	4,33	4,67	5,75	0,58
197	2,67	-1,33	5,33	2,22	3,00	0,67	3,00	3,67	2,58	-0,36
203	-1,67	-1,00	5,33	0,89	1,33	1,00	3,33	3,67	2,33	-1,44

4.2.3.3 Semi-automated evaluation of predefined tissue areas

Each histological IHC slide was digitally scanned with the Ventana DP200 scanner at 20x magnification. Whole slide images were analyzed using QuPath software[59], focusing on three preselected specific areas for each type of structure, as indicated in the Supplementary materials (Predefined reference areas section, Figure 6 and Figure 7). Areas containing artifacts were excluded from the analysis.

The maximum intensity values of the DAB signal within all selected areas were recorded in a spreadsheet. For each type of structure, a single value was obtained by calculating the mean of the three preselected areas' values. Subsequently, an overall mean value was calculated for both the positive structures category and the negative structures category. The difference between these two mean values was then computed and used to rank the protocol list (Table 10).

Table 10. *Results from the semi-automated evaluation of predefined tissue areas (final protocol in bold).*

Protocols ID	Results
212	2,059
210	1,816
197	1,459
211	1,419
205	1,316
203	1,146
207	0,981

4.2.3.4 PD-L1 E1L3N clone immunohistochemical protocol final selection

IHC staining protocols for PD-L1 using the E1L3N clone were evaluated through three different approaches as previously reported. Based on these evaluations, the three top-performing protocols were selected for further testing. Each protocol was applied to two different TNBCs, which were clinically evaluated as SP142 PD-L1-positive. This step aimed to verify the staining performance of each protocol on the target tissue, neoplastic breast carcinoma.

Following this comparative analysis, protocol 212 (Table 11) was selected for the study because it demonstrated an excellent signal-to-noise ratio and showed no evidence of non-specific background staining.

Table 11. *Immunohistochemistry final protocol (ID 212) for E1L3N clone on Ventana Benchmark Ultra.*

Characteristics	Details
Detection kit	OptiView
Deparaffinization	72°C
Cell conditioning	ULTRA CC1, 48 minutes at 99°C
Antibody dispensation	Manual
Pre-primary peroxidase inhibition	Selected
Primary antibody	1:100, 16 minutes at 36°C
OptiView HQ linker	8 minutes
OptiView multimer	8 minutes
OptiView amplification	Selected
H_2O_2 amplification	8 minutes
Multimer amplification	8 minutes
Nuclear counterstaining	Hematoxylin 2, 8 minutes
Post-counterstaining bluing	Bluing reagent, 4 minutes

4.2.4 PD-L1 immunohistochemical stainings of triple-negative breast cancer selected samples

For each patient, three histological slides were prepared. Two slides were used for PD-L1 IHC staining (E1L3N and SP142 clones), and one was stained with hematoxylin and eosin to be used as a morphological reference for PD-L1 evaluation and to confirm patient eligibility.

Each slide, as shown in Figure 3, includes the following 4 µm-thick sections:

- A tonsil section used as a staining reaction control.
- A section from the FFPE biopsy sample.
- A section from the selected FFPE resected tumor sample.

IHC staining was performed within seven days after slide preparation, using the Ventana BenchMark ULTRA platform. The specific staining protocols for the SP142 clone and for the E1L3N clone are detailed in Table 7 and in Table 11.

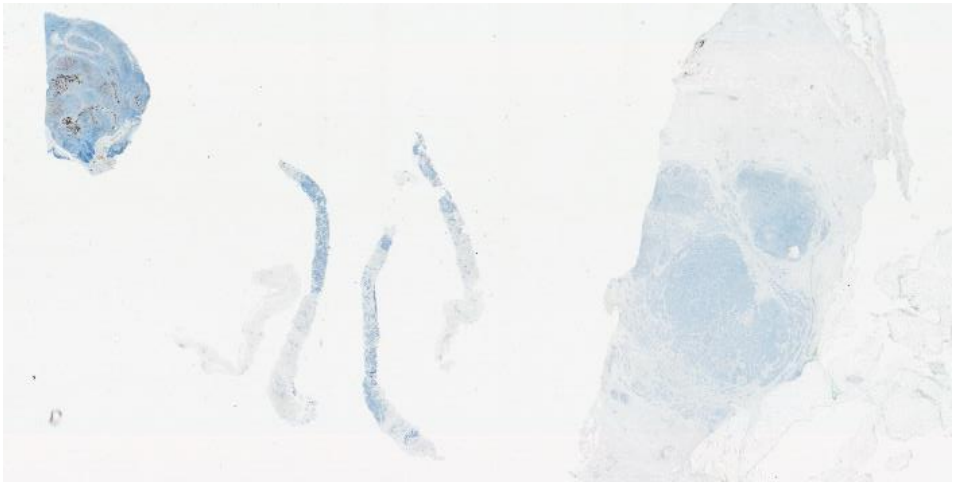

Figure 3. *Example of PD-L1 immunohistochemical slide (SP142 clone) with tonsil control section (upper left), biopsy section (center), and corresponding surgical resection section (right).*

4.3 PD-L1 IMMUNOHISTOCHEMICAL STAIN SCAN AND EVALUATION

All the slides were digitally scanned using the Aperio GT 450 DX slide scanner. Whole slide images (WSIs) of PD-L1 IHC-stained slides were reviewed using QuPath software, and both the IC score and the CPS were evaluated by a pathologist. All evaluations were conducted in a blind manner, allowed by the filename masking feature available in the QuPath software[60]. PD-L1 expression assessment on biopsy and resection specimens was performed in separate sessions to minimize potential bias.

4.4 SOFTWARE-ASSISTED MEASUREMENTS OF BIOPSY PARAMETERS

WSIs of biopsy slides were analyzed and measured using QuPath software[60]. For each case, the following parameters were recorded:

- Number of tissue fragments.
- Number of fragments containing neoplastic tissue.
- Estimated number of core biopsies performed, based on the length of the greatest fragment observed in the section.
- Number of tumor/stroma interfaces within the fragments.
- Total tumor length in the biopsy sample, calculated by summing all the lengths of the invasive tumor tissue across the fragments.
- Total tumor area in the biopsy sample, obtained by summing all the areas of invasive tumor tissue across the fragments.

Subsequently, the following values were calculated based on the previously collected data:

- Number of biopsies per centimeter of the greatest tumor dimension.
- Number of tumor/stroma interfaces per centimeter of the greatest tumor dimension.
- Total tumor length in the biopsy sample per centimeter of the greatest tumor dimension.
- Total tumor area in the biopsy sample per centimeter of the greatest tumor dimension.

All the results were stored in a spreadsheet in a pseudo-anonymized manner.

4.5 STATISTICAL ANALYSIS

Statistical analyses were performed using Jamovi software, an open-source graphical user interface for the R programming language. Descriptive statistics (mean, median, standard deviation, interquartile range) were calculated for all measured variables [61].

To address the primary objective of the study, Cohen's kappa coefficient (κ, with 95% confidence intervals) and percentage agreement were calculated to assess concordance of PD-L1 evaluations between biopsy and surgical specimens, using different scoring systems applied to specific antibody clones (IC score for SP142 and CPS for E1L3N, used as a surrogate for 22C3). Additional exploratory analyses were conducted for speculative purposes using scoring systems not specifically validated for the antibodies employed, between biopsies and resection specimens, and between biopsies and overall PD-L1 status. Overall, PD-L1 status was defined as positive when either the biopsy or the surgical specimen was positive, and negative when both were negative[62–64].

The diagnostic performance of biopsy-based PD-L1 assessment was evaluated by calculating sensitivity, specificity, positive predictive value (PPV), and negative predictive value (NPV), considering the surgical specimen evaluation as the reference standard[62,65,66].

To investigate the association between PD-L1 concordance (biopsy vs surgical specimen) and histologically measurable parameters on biopsy sections, univariate binomial logistic regression was performed for PD-L1 evaluation using IC score for SP142 and CPS for E1L3N[67]. Additionally, contingency tables were constructed applying arbitrary positivity cutoffs for biopsy-measured parameters, and Chi-square or Fisher's exact tests were used to assess associations.

The adopted cutoffs were:

- At least 2, 3, or 4 CNBs collected.
- At least 1 CNB per 1, 1.5, and 2 cm of tumor.
- At least 1, 2, 3, or 4 tumor/stroma interfaces present in the biopsy sample.
- Mean, first quartile, median, and third quartile of tumor length in the biopsy sample.
- Mean, first quartile, median, and third quartile of tumor length in the biopsy sample per cm of tumor dimension.
- Mean, first quartile, median, and third quartile of tumor area in the biopsy sample.
- Mean, first quartile, median, and third quartile of tumor area in the biopsy sample per cm of tumor dimension.

Finally, the cohort was stratified into concordant and discordant subgroups based on the agreement of PD-L1 status between biopsy and surgical specimens. For each clone, independent

samples two-sided t-tests were performed to compare biopsy-measured parameters between these two subgroups. A significance level of $p < 0.05$ was adopted for all tests.

5 UNPUBLISHED RESULTS

5.1 DESCRIPTIVE STATISTICS OF THE SAMPLE SPECIMENS

The study sample consisted of 49 female patients with a median greatest tumor dimension of 21 mm. Biopsies were performed with a median of 3 CNB samples per patient. In 63% of cases, at least one biopsy was obtained for every 1 cm of tumor dimension, with a median value of 1.33 CNB samples per centimeter of tumor dimension. The median number of tumor/stroma interfaces was 3 per patient, corresponding to a median of 1.43 interfaces per centimeter of tumor dimension. Biopsy samples showed a median total tumor length of 20.32 mm and 10.10 mm for every 1 cm of tumor dimension. The median tumor area was 15.04 mm^2, and 6.93 mm^2 per centimeter of tumor dimension. Further details on the measured variables are provided in Table 12.

Table 12. *Descriptive statistics of the sample specimens. Tumor dimension refers to the greatest dimension measured on the surgical resection specimen (Min: minimum; Max: maximum).*

Parameter	Mean	SE	Median	SD	IQR	Min	Max
Tumor dimension (mm)	26.20	2.53	21	17.69	17	6	100
Biopsies (estimate No.)	2.78	0.15	3	1.03	2	1	5
Biopsy fragments (No.)	4.02	0.29	4	2.05	3	1	9
Biopsy fragments with tumor (No.)	3.18	0.21	3	1.47	2	1	7
Biopsies per cm of tumor dimension (No.)	1.54	0.18	1.33	1.22	1.02	0.31	5.71
Interfaces (No.)	2.63	0.23	3	1.59	2	0	7
Interfaces per cm of tumor dimension (No.)	1.67	0.26	1.43	1.79	1.53	0.00	10.00
Tumor length in biopsy (mm)	20.79	1.69	20.32	11.81	17.06	3.91	52.79
Tumor length in biopsy per cm of tumor dimension (mm)	10.08	0.94	10.10	6.58	9.46	0.70	31.37
Tumor area in biopsy (mm^2)	16.83	1.81	15.04	12.66	12.63	2.11	78.10
Tumor area in biopsy per cm of tumor dimension (mm^2)	8.47	0.98	6.93	6.89	9.40	0.76	29.83

5.2 PD-L1 EXPRESSION PREVALENCE

For technical reasons, PD-L1 IHC staining was performed using the SP142 clone in 48 patients and the E1L3N clone in 43 patients. Overall, 42 patients were evaluated with both PD-L1 antibody clones. An example of PD-L1 IHC slide images stained with the SP142 and E1L3N clones is shown in Figure 4.

Using the SP142 clone and the IC score with a 1% cutoff, 8 patients (17%) were classified as positive on biopsy, whereas 19 patients (40%) were positive on the surgical specimen. Discordance between biopsy and surgical specimen was observed in 13 cases (27%), including 12 patients (25%) who were negative on biopsy but positive on the surgical specimen, and 1 patient (2%) who was positive on biopsy but negative on the surgical specimen. Considering positivity in at least one specimen type, 20 patients (42%) showed a PD-L1-positive sample.

Similarly, PD-L1 assessment using the E1L3N clone and a CPS cutoff of 10 revealed that 9 patients (21%) were positive on biopsy, 11 patients (26%) were positive on the surgical specimen, and 6 cases (14%) were discordant. Among those, 4 patients (9%) were negative on biopsy but positive on the surgical specimen, and 2 cases (5%) were positive on biopsy but negative on the surgical specimen. Considering positivity in at least one specimen type, 13 patients (30%) showed a PD-L1-positive sample.

In the study cohort, the PD-L1 status on biopsy showed that 6 patients (14%) were positive for both tests (IC score with SP142 and CPS with E1L3N), 31 patients (74%) were negative for both, and 5 patients (12%) showed discordant results between the two assays.

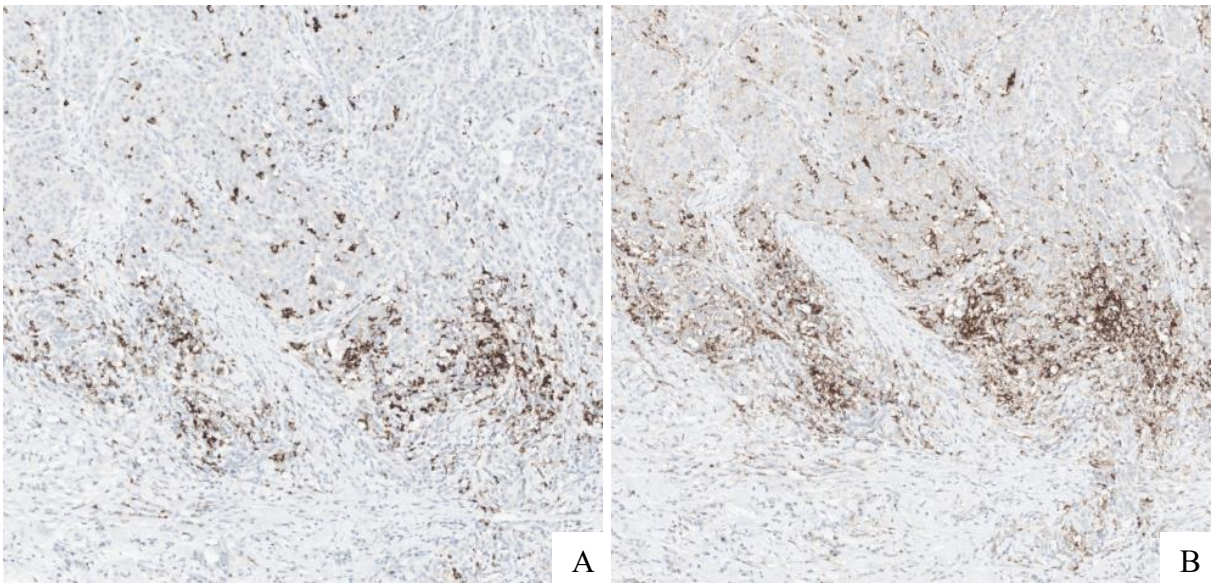

Figure 4. *Comparison of PD-L1 immunohistochemical staining in the same TNBC area using two different clones (digitally scanned with 20x objective). A) SP142 clone; B) E1L3N clone.*

5.3 PD-L1 EXPRESSION CONCORDANCE TESTS

The concordance between the two main PD-L1 evaluation methods (IC score for the SP142 clone and CPS for the E1L3N clone) was 88% on biopsy specimens (κ = 0.632), 83% on surgical specimens (κ = 0.624), and 86% for overall PD-L1 status (κ = 0.692) (Table 13). When comparing biopsy and surgical specimens, concordance was 73% for the SP142 clone evaluated with IC score (κ = 0.371) and 86% for the E1L3N clone evaluated with CPS (κ = 0.610), as shown in Figure 5.

Among the concordance tests performed between biopsy and surgical specimens, and between biopsy and overall PD-L1 status (Figure 5), using different combinations of scoring systems and clones, the highest agreement with IC/SP142 evaluations was observed for CPS/E1L3N on biopsy samples, with concordance rates of 79% (κ = 0.504) for surgical specimens and 81% (κ = 0.573) for overall PD-L1 status. Regarding CPS/E1L3N evaluations, the strongest concordance was achieved when comparing biopsy assessment using the same CPS/E1L3N combination, with agreement rates of 86% (κ = 0.610) for surgical specimens and 91% (κ = 0.758) for overall PD-L1 status.

Additional exploratory concordance analysis results are reported in Figure 5.

Table 13. *PD-L1 expression concordance analysis using Cohen's Kappa test (bio = biopsy; res = surgical resection specimen; status = overall PD-L1 status).*

Tests		N	Agreement	Kappa	p-value
CPS E1L3N bio	IC SP142 bio	42	88%	0.632	<.001
CPS E1L3N res	IC SP142 res	42	83%	0.624	<.001
IC SP142 status	CPS E1L3N status	42	86%	0.692	<.001

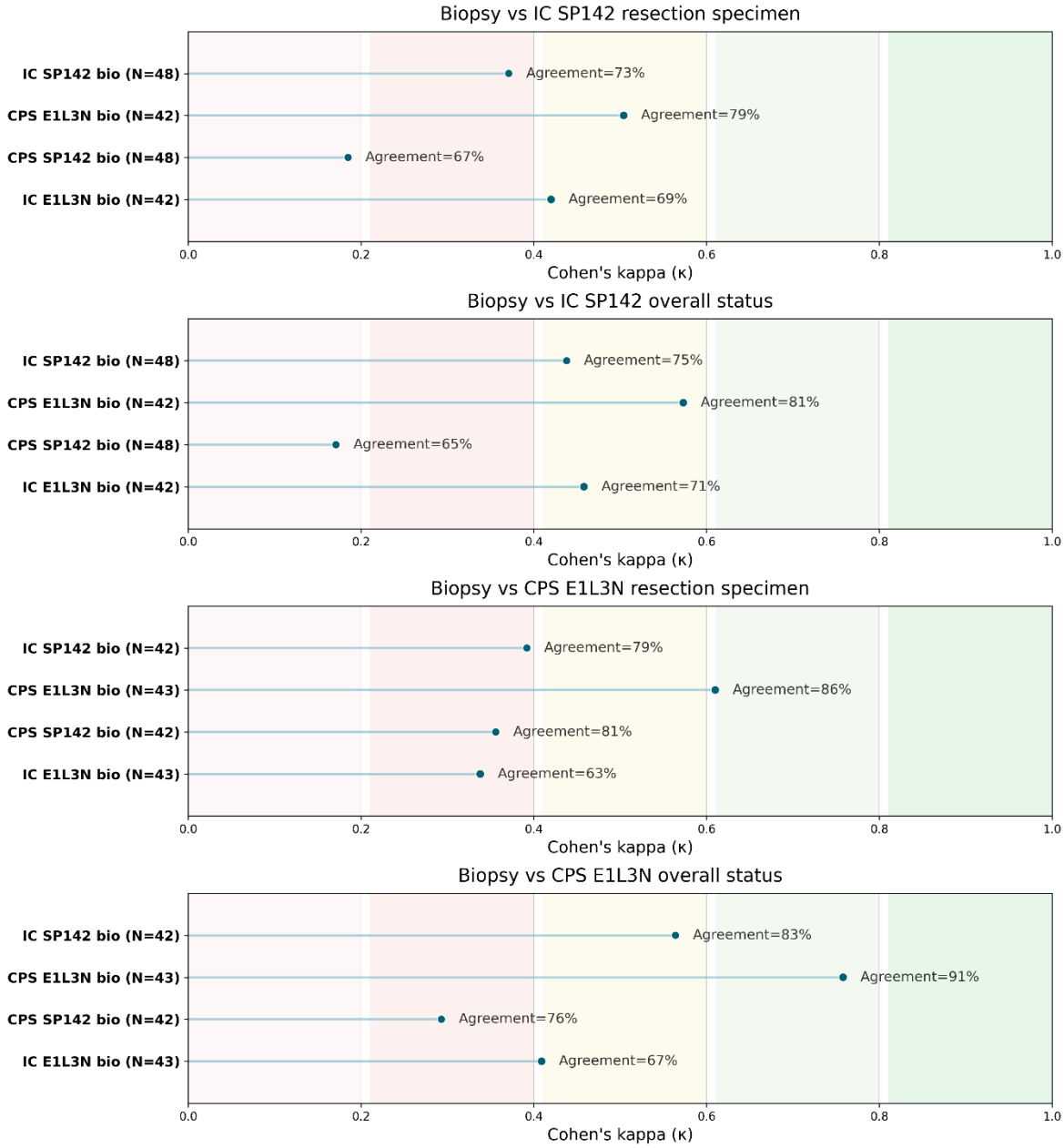

Figure 5. *Forest plot of agreement (Cohen's κ) across biopsy and resection specimen or overall PD-L1 status (bio = biopsy; res = surgical resection specimen; status = overall biopsy and resection specimen status). Background bands show Landis & Koch's interpretation: κ < 0.00: Poor; 0.00–0.20: Slight; 0.21–0.40: Fair; 0.41–0.60: Moderate; 0.61–0.80: Substantial; 0.81–1.00: Almost perfect. Labels report agreement (%) and N; p-values <0.05 for all tests.*

5.4 PREDICTIVE PERFORMANCE OF BIOPSY-BASED PD-L1 ASSESSMENT

PD-L1 expression on biopsies was compared with surgical specimens as a reference standard for both PD-L1 evaluation assays. Using the SP142 clone with an IC score (cutoff 1%), biopsy assessment showed a sensitivity of 36.8%, specificity of 96.6%, PPV of 87.5%, and NPV of 70.0%. Conversely, PD-L1 evaluation using CPS with the E1L3N clone (cutoff 10) yielded a sensitivity of 63.6%, specificity of 93.8%, PPV of 77.8%, and NPV of 88.2% (Table 14 and Table 15).

Subsequently, possible combinations of clone and scoring system were explored to assess the predictive performance of PD-L1 expression on biopsy specimens. It was found that none of the analyses performed provided a reliable predictor of PD-L1 expression on surgical specimens. However, notable results were obtained from two specific configurations. First, regarding the prediction of IC/SP142 status on surgical specimens, a PPV of 100% was achieved by the CPS/SP142 combination on biopsies, although positivity was observed in only 3 out of 48 patients (Table 14). Conversely, an NPV of 93.3% was demonstrated by the IC/E1L3N combination on biopsies, with 14 negative cases out of 42 total surgical resections being correctly identified, and only 1 false negative result recorded. Significant predictive value was also shown by these same two biopsy-based tests when evaluated against the CPS/E1L3N status on surgical specimens, specifically a PPV of 100.0% was again achieved by CPS/SP142 on biopsies (3 positive cases out of 42), while an NPV of 100.0% was reached by IC/E1L3N on biopsies, with 16 negative cases out of 43 total patients being correctly identified (Table 15).

As an exploratory analysis, an interchangeability test was conducted to determine whether PD-L1 evaluation on biopsy samples could be considered equivalent when assessed using the two assays (CPS/E1L3N and IC/SP142). The results showed that complete concordance between the two approaches was not achieved. When each assay was used as a reference for the other, both methods demonstrated high specificity (>91%) and high negative predictive value (NPV >91%), but low sensitivity (≤75%) and low positive predictive value (PPV ≤75%) (Table 16).

Further results on sensitivity, specificity, and predictive performance of the above-mentioned and other tests are reported in Tables Table **14**-Table **16**.

Table 14. *Sensitivity, specificity, and predictive performance of PD-L1 evaluation on biopsy samples compared to IC score with SP142 on surgical specimens or overall PD-L1 status as reference standard (bio = biopsy; res = surgical resection specimen; status = overall PD-L1 status; PPV = positive predictive value; NPV = negative predictive value).*

Test	Reference standard	Sensitivity	Specificity	PPV	NPV
IC SP142 bio	IC SP142 res	36.8%	96.6%	87.5%	70.0%
CPS E1L3N bio		50.0%	96.2%	88.9%	75.8%
CPS SP142 bio		15.8%	100.0%	100.0%	64.4%
IC E1L3N bio		93.8%	53.8%	55.6%	93.3%
IC SP142 bio	IC SP142 status	40.0%	100.0%	100.0%	70.0%
CPS E1L3N bio		52.9%	100.0%	100.0%	75.8%
CPS SP142 bio		15.0%	100.0%	100.0%	62.2%
IC E1L3N bio		94.1%	56.0%	59.3%	93.3%

Table 15. *Sensitivity, specificity, and predictive performance of PD-L1 evaluation on biopsy samples compared to CPS with E1L3N on surgical specimens or overall PD-L1 status as reference standard (bio = biopsy; res = surgical resection specimen; status = overall PD-L1 status; PPV = positive predictive value; NPV = negative predictive value).*

Test	Reference standard	Sensitivity	Specificity	PPV	NPV
CPS E1L3N bio	CPS E1L3N res	63.6%	93.8%	77.8%	88.2%
IC SP142 bio		45.5%	90.3%	62.5%	82.4%
CPS SP142 bio		27.3%	100.0%	100.0%	79.5%
IC E1L3N bio		100.0%	50.0%	40.7%	100.0%
IC SP142 bio	CPS E1L3N status	53.8%	96.6%	87.5%	82.4%
CPS E1L3N bio		69.2%	100.0%	100.0%	88.2%
CPS SP142 bio		23.1%	100.0%	100.0%	74.4%
IC E1L3N bio		100.0%	53.3%	48.1%	100.0%

Table 16. *Sensitivity, specificity, and predictive performance of PD-L1 evaluation on biopsy samples (bio = biopsy; PPV = positive predictive value; NPV = negative predictive value).*

Test	Reference standard	Sensitivity	Specificity	PPV	NPV
CPS E1L 3N bio	IC SP142 bio	75.0%	91.2%	66.7%	93.9%
IC SP142 bio	CPS E1L3N bio	66.7%	93.9%	75.0%	91.2%
IC E1L3N bio	IC SP142 bio	100.0%	44.1%	29.6%	100.0%
CPS SP142 bio	CPS E1L3N bio	33.3%	100.0%	100.0%	84.6%

5.5 ASSOCIATION ANALYSIS BETWEEN BIOPSY-MEASURED PARAMETERS AND PD-L1 EXPRESSION CONCORDANCE

From the analysis of the parameters measured in biopsy sections, no statistically significant results emerged from the univariate binomial logistic regression tests, both for the SP142 clone evaluated with IC score (Table 17) and for the E1L3N clone assessed with CPS (Table 18).

Table 17: *Univariate logistic binomial regression analysis of predictors of IC score concordance (SP142 clone). AUC = ROC curve AUC.*

Predictor	Odds ratio	AUC	p-value
Biopsies (estimate No.)	1.210	0.541	0.539
Biopsies per cm of tumor dimension (No.)	0.712	0.603	0.277
Interfaces per cm of tumor dimension (No.)	0.748	0.613	0.239
Tumor length in biopsy (mm)	1.015	0.553	0.572
Tumor length in biopsy per cm of tumor dimension (mm)	0.945	0.561	0.274
Tumor area in biopsy (mm^2)	0.989	0.508	0.678
Tumor area in biopsy per cm of tumor dimension (mm^2)	0.919	0.602	0.129

Table 18: *Univariate logistic binomial regression analysis of predictors of CPS concordance (E1L3N clone). AUC = ROC curve AUC.*

Predictor	Odds ratio	AUC	p-value
Biopsies (estimate No.)	0.630	0.609	0.214
Biopsies per cm of tumor dimension (No.)	0.596	0.640	0.182
Interfaces per cm of tumor dimension (No.)	0.741	0.595	0.278
Tumor length in biopsy (mm)	1.003	0.527	0.908
Tumor length in biopsy per cm of tumor dimension (mm)	0.953	0.559	0.399
Tumor area in biopsy (mm^2)	0.995	0.465	0.862
Tumor area in biopsy per cm of tumor dimension (mm^2)	0.956	0.554	0.422

Contingency tables were constructed to evaluate the association between PD-L1 status concordance and the measured biopsy parameters. Concordance was determined for both the IC/SP142 and CPS/E1L3N assays (biopsy vs surgical specimen comparison), and arbitrary positivity cutoffs were applied to the parameters. A chi-square or Fisher's exact test was performed on these tables, without evidence of a statistically significant association between the analyzed groups (Supplementary materials, Table 25).

Finally, the cohort was divided into two subgroups based on PD-L1 status concordance between biopsy and surgical specimens with the SP142 clone (Supplementary materials, Table 26). These subgroups were compared using a two-sided independent t-test applied to the parameters measured in biopsies (Supplementary materials, Table 28). No statistically significant differences were observed between the two groups. The same analysis performed on subgroups based on PD-L1 status evaluated with the E1L3N clone (Supplementary materials, Table 27) also showed no statistically significant differences (Supplementary materials, Table 28).

6 DISCUSSION

6.1 METHODOLOGICAL APPROACH TO PD-L1 IMMUNOHISTOCHEMISTRY PROTOCOL SELECTION AND OPTIMIZATION FOR TRIPLE-NEGATIVE BREAST CANCER

In this study, we used the E1L3N clone, an anti-PD-L1 antibody widely used in research settings, for which only a single validated IHC protocol is currently available in the literature. That protocol was originally developed for NSCLC on the Leica Bond MAX platform[53], and has not yet been formally validated for TNBC.

The laboratory where we performed IHC staining did not have access to the Leica platform. Consequently, we selected alternative IHC protocols for the E1L3N clone from the literature that demonstrated reliable performance on the Ventana BenchMark ULTRA platform, which was available in the laboratory. However, these selected protocols were often incompletely reported, lacking essential methodological details.

Due to the unavailability of histological sections and clinical data from TNBC cases included in pivotal trials of atezolizumab or pembrolizumab, we were unable to test candidate protocols on such reference material. This limitation prevented us from determining which protocol would provide optimal sensitivity and specificity to identify patients who respond to therapy. Therefore, our aim was not to develop an IHC protocol with predictive capability for pembrolizumab response in TNBC, but rather to optimize PD-L1 staining quality, maximizing specific signal intensity while minimizing background and non-specific staining. Consequently, we designed a stepwise testing strategy to select the most suitable protocol among the available candidates. To achieve this, we tested a novel methodology for IHC protocol selection using tonsil tissue sections as reference material. Tonsil tissue contains a variety of PD-L1-positive structures with variable antigen expression, including squamous epithelium and lymphoid follicles with germinal centers, as well as PD-L1-negative structures such as fibrous stroma, vascular structures, and salivary glands. The three best-performing protocols identified through the selection methods tested on tonsil tissue (i.e., *ranking by pathologists*, *optical evaluation of predefined tissue areas*, and *semi-automated analysis*) were subsequently tested on TNBC sections, and protocol ID 212 was ultimately selected as the final IHC protocol for the E1L3N clone. However, as the number of cases analyzed increased, we observed an unexpected granular cytoplasmic staining in tumor cells in some samples. This non-specific positivity appeared in certain surgical specimens and, in a subset of these cases, also in corresponding biopsy sections, and was absent in the sections stained with the SP142 clone. Notably, this staining pattern had already been described in a recent study. Therefore, this signal was

interpreted as non-specific and excluded from PD-L1 scoring, in accordance with Erick et al[52]. Fortunately, this artifact was easily recognizable in most cases and interfered with scoring in only few instances. This limitation underscores the need to reassess the performance of the selected protocol and suggests that future evaluations should include a larger number of target tissues. In our context, this would involve a broader panel of TNBC samples. A promising strategy could be the development of a tissue microarray (TMA) comprising a large number of TNBC samples with variable PD-L1 expression, along with normal breast tissue, breast carcinoma in situ, non-neoplastic tissues (e.g., liver, lung, decalcified bone), and breast metastases (e.g., bone metastases decalcified with different solutions, lymph node metastasis, cerebral metastases, pleural metastases, liver metastases). This strategy would enable a comprehensive assessment of staining performance across different settings, explore antigen expression in various tissue components, and help exclude protocols prone to non-specific staining.

The challenge of optimizing new IHC protocols for novel antibodies remains open. Two novel IHC protocol selection methods were developed in this study to increase the objectivity of evaluations and reduce the need for highly specialized IHC personnel. While the *Ranking by pathologists* method, the usual approach, requires a pathologist with extensive expertise in IHC staining optimization, the *Optical staining evaluation of predefined tissue areas* method enables a more objective assessment through a predefined intensity scale. That method could be performed by less experienced staff, like a general pathologist or a pathologist in training. Finally, the *Semi-automated evaluation of predefined tissue areas* method does not require highly qualified personnel; a single operator with basic histology and pathology knowledge could be sufficient to select specific predefined areas and replicate the selection in consecutive serial sections of the same tissue sample, as the evaluation is performed by dedicated software, like QuPath. Therefore, this method could be performed by non-pathologist personnel, such as biologists or biotechnologists. Although both novel IHC protocol selection methods identified the same protocol as the best in this study, and this choice was supported by the *Ranking by pathologists* method, it remains necessary to confirm the effectiveness of these approaches through a more objective comparison. A promising strategy would be comparing the preference of an expert in IHC protocol optimization with the two proposed methods, using an antibody that targets an antigen quantifiable by an alternative technique, thereby providing objective reference values. This approach would allow the comparison of the results obtained through different selection methods with measurable outcomes, thereby determining whether the new methods can achieve performance comparable to an expert-driven optimization.

6.2 REPRESENTATIVENESS OF PD-L1 IMMUNOHISTOCHEMICAL EVALUATION

According to the latest Italian guidelines for the management of aTNBC, PD-L1 expression assessment is performed using two companion diagnostic assays: the SP142 clone evaluated with the IC score to predict response to atezolizumab, and the 22C3 clone assessed with the CPS to determine eligibility to pembrolizumab treatment. In cases where a patient presents an aTNBC as initial diagnosis, the only tissue available for PD-L1 evaluation is usually the CNB of the primary tumor, supplemented by a small biopsy of a metastatic site in cases of initial mTNBC presentation. Therefore, having a reliable method to assess PD-L1 expression on limited tissue samples is of paramount importance.

Recent retrospective studies have investigated PD-L1 IHC expression on biopsy specimens compared to corresponding surgical samples, reporting highly variable results. Focusing on the SP142 clone evaluated using the IC score with a 1% cutoff, the official criterion for atezolizumab eligibility in TNBC patients, three recent studies showed PD-L1 positivity rates on biopsy samples of 11% (Noske et al.)[68], 28% (Zdrenka et al.)[56], and 30% (Dobritoiu et al.)[69]. In our study, PD-L1 positivity on biopsy specimens was 17%, falling between those values. When analyzing surgical specimens from the same patients, all these studies observed a marked increase in positivity rates, reaching 53% (Noske et al.)[68], 51% (Zdrenka et al.)[56], and 52% (Dobritoiu et al.)[69]. Lower positivity rates have been reported in studies that evaluated all patient specimens collectively (overall PD-L1 positivity), such as the IMpassion130 trial, which led to the accelerated approval of atezolizumab for aTNBC. In that study, PD-L1 testing was performed on multiple samples from different anatomical sites and across various specimen types (i.e., CNB, excisional, incisional, punch, and forceps biopsies), resulting in an overall PD-L1 status positivity rate of 40.9%[32]. Another study that analyzed pooled samples was conducted by Al-Jussani et al., reporting an overall PD-L1 positivity rate of 36.7% [70]. In comparison, our study demonstrated a PD-L1 positivity rate of 40% on surgical samples and an overall PD-L1 status positivity rate of 42%, which falls between the previously reported values. Regarding the 22C3 clone evaluated using CPS with a cutoff of 10, the official criterion for pembrolizumab eligibility, a single study (Noske et al.) reported a PD-L1 positivity rate of 23.5% on CNB specimens[68]. This value is comparable to our finding of 21% PD-L1-positivity in biopsy samples analyzed with the E1L3N antibody, used as a surrogate of the 22C3 clone. When analyzing the corresponding surgical specimens, we observed a PD-L1-positivity rate slightly increased to 26% with the E1L3N clone, whereas Noske et al. reported positivity in 5 out of 29 cases (17%) with the 22C3 clone. In our cohort, the overall PD-L1 status positivity

for PD-L1 using the E1L3N clone and CPS was 30%, a little lower than the 38.1% reported in the KEYNOTE-355 trial, which supported pembrolizumab approval for aTNBC. In that study, PD-L1 expression was evaluated with the 22C3 clone and CPS, performing tests on multiple samples per patient, from different anatomical sites, and with various specimen types[37].

The data obtained in our study were consistent with previously published findings and confirmed substantial differences in PD-L1 positivity rate between biopsy specimens and corresponding surgical resections.

Based on the Landis and Koch's interpretation of Cohen's Kappa[64], the agreement between biopsy and surgical specimens for SP142 (IC score) was classified as *fair* ($\kappa = 0.371$), with 27% discordant cases, whereas the agreement for E1L3N (CPS) was *substantial* ($\kappa = 0.610$), with 14% discordant cases. Agreement results were slightly higher when biopsies were compared to the overall PD-L1 status, showing *moderate* agreement ($\kappa = 0.438$) for SP142 (IC score) with 21% discordant cases, and *substantial* agreement ($\kappa = 0.758$) for E1L3N (CPS) with 9% discordant cases. Although the E1L3N clone cannot be directly interpreted as the 22C3 clone, its performance appears more robust, particularly in the context of pembrolizumab eligibility testing. These concordance values indicate that PD-L1 evaluation on CNB is not sufficiently reliable for predicting the PD-L1 status of the surgical specimen, and is only slightly better at estimating the overall PD-L1 status. The discordance is particularly pronounced for IC score assessment with the SP142 clone, the designated eligibility test for atezolizumab.

Considering the clinical setting where the biopsy is the only tissue available for PD-L1 testing, our comparison with surgical specimens (as the reference standard) revealed significant discrepancies. Specifically, for the IC/SP142 assay, among patients classified as negative on biopsy, 30% were in fact false negatives and would have been denied atezolizumab treatment. Similarly, using the CPS/E1L3N combination (as a surrogate for 22C3), among patients classified as negative on biopsy, 11.8% were false negatives and would have been incorrectly excluded from pembrolizumab therapy.

These findings highlight the clinical risk of missing PD-L1-positive identification for the eligibility to ICI therapy when relying solely on biopsy-based PD-L1 assessment, underscoring the importance of extending PD-L1 evaluations on multiple specimens whenever possible, or even developing new tests with greater reliability on biopsy samples.

Given the suboptimal results obtained by the concordance tests between biopsy and surgical specimens, we conducted additional exploratory analyses to assess whether PD-L1 expression assessed on biopsy specimens could provide meaningful predictive insights into overall PD-L1 status. These analyses revealed some interesting results.

First, regarding the estimation of overall PD-L1 status using the SP142 clone with the IC score (the standard for atezolizumab eligibility), the alternative biopsy-based CPS/E1L3N test demonstrated a PPV of 100%. This suggests that a positive result with this method ensures the accurate identification of eligible patients. Furthermore, the IC/E1L3N combination on biopsies showed a high NPV of 93.3%, effectively excluding non-responders with only one false negative recorded among 15 negative biopsies. In contrast, while the standard IC/SP142 biopsy test also maintained a PPV of 100%, its NPV was significantly lower at 70%, resulting in the incorrect exclusion of 12 out of 40 PD-L1-negative patients from potential therapy.

Similarly, when considering overall PD-L1 status using the E1L3N clone with the CPS method (22C3 surrogate test), the alternative IC/E1L3N biopsy test achieved an NPV of 100%, ensuring the accurate determination of negativity. Conversely, the CPS/E1L3N test on biopsies showed a reduced NPV of 88.2%, leading to the misclassification of 4 out of 34 negative biopsies.

Collectively, these findings suggest that alternative combinations of scoring algorithms and antibody clones, beyond those currently recommended, warrant further investigation in clinical studies. Such approaches could help define more reliable strategies for estimating overall PD-L1 status in TNBC biopsies and, ultimately, improve the prediction of response to ICIs.

Beyond the predictive performance of alternative scoring and clone combinations, practical considerations regarding assay availability and cost are also pivotal in clinical decision-making. It is important to note that, given the low incidence of aTNBC, implementing the specific SP142 assay may not be economically sustainable for small- to medium-sized laboratories. Notably, a recent Italian national survey reported that approximately one-third of the 128 centers surveyed lacked access to the SP142 clone[71]. Consequently, this limitation compels these institutions to rely on outsourcing the test, inevitably delaying treatment initiation for patients with aTNBC or mTNBC.

As highlighted in literature, SP142 cannot simply be replaced by other clones such as 22C3, SP263, or E1L3N, due to the lack of interchangeability demonstrated in concordance studies[46,72], and our findings confirm these observations. However, based on the superior negative predictive value demonstrated by the IC/E1L3N combination compared to the standard IC/SP142 biopsy test, we propose the use of the E1L3N clone evaluated with IC score as a reliable “rule-out” test. This strategy would enable cost-effective screening in small- to medium-sized laboratories, allowing for the immediate exclusion of patients who do not require atezolizumab, thereby accelerating therapy initiation. Consequently, external consultations (and the associated delays) would be restricted strictly to cases showing IC score positivity with E1L3N. While promising, these findings are derived from a limited sample size and require formal validation in larger cohorts before clinical implementation. Furthermore, given the

widespread availability of other clinically validated clones already used in the aTNBC setting for pembrolizumab eligibility (e.g., 22C3 and SP263[71]), it would be of great interest to investigate their potential as similar screening tools. This approach would avoid the burden of setting up the E1L3N test, allowing laboratories to rely on antibodies they already possess.

Addressing the imperfect concordance of PD-L1 expression between biopsy and surgical specimens, we investigated whether specific measured biopsy parameters could serve as quality indicators to predict the reliability of PD-L1 assessment on biopsy. Previous literature, notably studies by Sun et al. and Tamaki et al.[73,74], recommends obtaining at least four core needle biopsies (CNBs) to ensure accurate diagnostic and prognostic profiling in breast carcinoma. In our cohort, the median number of CNBs was three, with 63% of cases presenting at least one CNB per centimeter of tumor size. To further investigate this analysis, we also evaluated the tumor-stroma interface, a critical site for PD-L1-positive inflammatory infiltrates[69]. Specifically, for each biopsy specimen we quantified the number of cores obtained, the number of tumor-stroma interfaces, the linear extent of invasive carcinoma, and the total invasive tumor area, also normalizing these parameters to tumor size. However, none of the analyzed variables demonstrated a significant ability to predict the representativeness of the biopsy result compared to the surgical specimen, even when the data were stratified by predefined cutoffs, including the recommended four-core threshold[73,74]. A possible explanation for the lack of statistical significance may be the limited sample size of our study. To eliminate confounding factors associated with neoadjuvant chemotherapy, we restricted our analysis exclusively to chemotherapy-naive patients. This stringent selection criterion, combined with the low incidence of TNBC, significantly limited the available study population. Therefore, although this was a multicentric study (involving four medical centers in Piedmont) with both retrospective and prospective enrollment, our final cohort consisted of 49 patients. This sample size is consistent with other recent investigations[68,70], notwithstanding that some of these studies employed less rigorous selection criteria and focused on a single antibody clone[56,70]. To address the limitations of this study, increasing the sample size and incorporating multiple PD-L1 staining evaluations by experienced pathologists from high-volume TNBC centers, as performed by Dobritoiu et al., would strengthen the conclusions. This approach could potentially allow for the identification of predictive factors regarding the representativeness of PD-L1 assessment on biopsy specimens[69].

In the meantime, one practical suggestion emerging from this study is to perform PD-L1 testing on all available tissue material (e.g., archived samples, metastatic locations) to maximize the likelihood of detecting PD-L1 positivity, particularly considering the type of specimens used in pivotal clinical trials of ICIs in TNBC[32,37]. Furthermore, a re-biopsy could be considered in

cases of initial PD-L1 negativity, particularly when the biopsy contains only a small amount of invasive tumor tissue. This approach is consistent with the suggestion by Dobritoiu et al., who requested additional tissue for PD-L1 assessment when the initial sample was limited and subsequently evaluated overall PD-L1 expression across all tested tissue (initial and repeated biopsies). Their findings showed that 23.6% of retested cases were positive for the IC score using SP142[69]. This strategy could improve the accuracy of PD-L1 estimation compared to surgical specimens, although it would inevitably delay the treatment initiation.

To overcome this challenge, a revised clinical workflow is warranted. First, in alignment with consensus guidelines on preoperative diagnostic procedures for breast lesions, we advocate for routine, extensive biopsy sampling. Specifically, we recommend obtaining a minimum of 4-6 CNBs from spatially distinct tumor areas using a 12-14 gauge needle, particularly for lesions eligible for neoadjuvant therapy[75]. Furthermore, we propose implementing reflex PD-L1 testing immediately upon TNBC diagnosis, followed by an accelerated staging pathway in case of negative results. In the setting of advanced or metastatic disease, priority should be given to urgent re-biopsy of the primary tumor and sampling of accessible metastatic sites, disfavoring immunologically "protected" sites such as the liver[69]. Re-evaluating prognostic factors on these fresh samples allows a more accurate assessment and facilitates timely therapeutic intervention.

7 CONCLUSIONS

This study highlights the critical challenge of PD-L1 assessment in TNBC when limited to diagnostic CNB specimens. We indirectly confirmed that PD-L1 expression is spatially heterogeneous and that relying solely on CNBs significantly underestimates PD-L1 status compared to surgical specimens and overall PD-L1 status. This discordance poses a concrete clinical risk, potentially excluding a significant proportion of eligible patients from ICI therapy, particularly when using the SP142 assay.

While no specific biopsy parameters were found to predict the reliability of PD-L1 evaluation, our data suggest a novel, practical utility for the E1L3N clone. Given its high NPV, E1L3N assessment using the IC score shows promise as a cost-effective rule-out test on biopsy. This strategy would allow smaller laboratories to reliably exclude non-eligible patients, reserving the more expensive and less available SP142 assay solely for confirming positive screening results.

Ultimately, until more robust predictive biomarkers for response to ICIs are validated, we propose a shift in the diagnostic paradigm: implementing reflex PD-L1 testing at TNBC diagnosis on all available samples to prompt immediate re-biopsy in cases of initial negativity, for the advanced or metastatic setting. These measures are essential to prevent treatment delays and ensure that every patient with aTNBC or mTNBC receives the most accurate evaluation for immunotherapy eligibility.

8 LIST OF PUBLICATIONS

- Ivaldi, M., Giacometti, L., & Conversi, D. (2023). Quantitative Electroencephalography: Cortical Responses under Different Postural Conditions. *Signals*, *4*(4), 708-724. https://doi.org/10.3390/signals4040039
- Erculiani, M., Poluzzi, F., Mottadelli, G., Felici, E., Ml, N., Caraccia, M., Grandi, A., Casella, S., Giacometti, L., Montobbio, G., Ceccherini, I., Di Marco, E., Bonaretti, C., Biassoni, R., Squillario, M., Pietrantoni, A., Villanacci, V., & Pini Prato, A. (2023). A unicentric cross-sectional observational study on chronic intestinal inflammation in total colonic aganglionosis: beware of an underestimated condition. *Orphanet journal of rare diseases*, *18*(1), 339. https://doi.org/10.1186/s13023-023-02958-1
- Pini Prato, A., Erculiani, M., Novi, M. L., Caraccia, M., Grandi, A., Casella, S., Giacometti, L., Montobbio, G., & Mottadelli, G. (2024). Delayed diagnosis in Hirschsprung disease. *Pediatric surgery international*, *40*(1), 65. https://doi.org/10.1007/s00383-024-05657-5
- Pini Prato, A., Mottadelli, G., Bertolino, A., Giacometti, L., Casella, S., Novi, M., & Erculiani, M. (2025). Unicentric Series of 82 Consecutive Patients With Ultralong Hirschsprung Disease: How Experience Leads Management. *Journal of pediatric surgery*, *60*(6), 162283. https://doi.org/10.1016/j.jpedsurg.2025.162283

9 SUPPLEMENTARY MATERIALS

9.1 VISUAL BASIC FOR APPLICATIONS SCRIPTS

Script 1. *Estrogen receptor extraction function.*

```
Function EstRec(testo As String) As String

    Dim temp As String

    temp = Mid(testo, InStr(1, testo, "estrogen", vbTextCompare), 70)


    If InStr(1, temp, "positiv", vbTextCompare) > 0 Then
        Estrogeni = "Positivo"
    ElseIf InStr(1, temp, "negativ", vbTextCompare) > 0 Then
        Estrogeni = "Negativo"
    Else
        Estrogeni = "NULL"
    End If


End Function
```

Script 2*. Progesterone receptor extraction function.*

```
Function ProgRec(testo As String) As String

    Dim temp As String

    temp = Mid(testo, InStr(1, testo, "progest", vbTextCompare), 70)


    If InStr(1, temp, "positiv", vbTextCompare) > 0 Then
        Progesterone = "Positivo"
    ElseIf InStr(1, temp, "negativ", vbTextCompare) > 0 Then
        Progesterone = "Negativo"
    Else
        Progesterone = "NULL"
    End If


End Function
```

Script 3. *HER2 extraction script function.*

```
Function HerTwo(text As String) As Integer

    Dim temp As String
    Dim temp2 As String

    temp = Mid(text, InStr(1, text, "4B5", vbTextCompare), 200)

    If InStr(1, temp, "score", vbTextCompare) > 0 Then
        temp2 = Mid(temp, InStr(1, temp, "score", vbTextCompare), 14)

        If InStr(1, temp2, "0", vbTextCompare) Or InStr(1, temp2,
"negativ", vbTextCompare) Then
            HerTwo = 0

        ElseIf InStr(1, temp2, "1", vbTextCompare) Then
            HerTwo = 1

        ElseIf InStr(1, temp2, "2", vbTextCompare) Or InStr(1, temp2,
"equiv", vbTextCompare) Then
            HerTwo = 2

        ElseIf InStr(1, temp2, "3", vbTextCompare) Or InStr(1, temp2,
"positiv", vbTextCompare) Then
            HerTwo = 3

        End If

    Else
        HerTwo = "NULL"

    End If


End Function
```

Script 4. *TNBC evaluation script function.*

```
Function TNBC(ER As String, PR As String, HerTwo As Integer) As String

    If (StrComp(ER, "Negativo", vbTextCompare) = 0 And StrComp(PR,
"Negativo", vbTextCompare) = 0) Then

        If HerTwo < 2 Then
            TNBC = "TNBC"

        ElseIf HerTwo = 2 Then
            TNBC = "Vedi ISH"

        ElseIf HerTwo = 3 Then
            TNBC = "Her2 POS"

        End If

    ElseIf (StrComp(ER, "Positivo", vbTextCompare) = 0 Or StrComp(PR,
"Positivo", vbTextCompare) = 0) Then
        TNBC = "Luminal"

    End If

End Function
```

9.2 IMMUNOHISTOCHEMISTRY PROTOCOLS

Table 19. *Immunohistochemistry protocol (ID 197) for E1L3N clone on Ventana Benchmark Ultra.*

Characteristics	Details
Detection kit	UltraView
Deparaffinization	72°C
Cell conditioning	ULTRA CC1, 36 minutes at 99°C
Antibody dispensation	Manual
Primary antibody	1:100, 60 minutes at 36°C
Amplification	Rabbit antibody amplification
UltraWash	Selected
Nuclear counterstaining	Hematoxylin 2, 8 minutes
Post-counterstaining bluing	Bluing Reagent, 4 minutes

Table 20. *Immunohistochemistry protocol (ID 207) for E1L3N clone on Ventana Benchmark Ultra.*

Characteristics	Details
Detection kit	UltraView
Deparaffinization	72°C
Cell conditioning	ULTRA CC1, 64 minutes at 95°C
Antibody dispensation	Manual
Primary antibody	1:100, 44 minutes at 39°C
Amplification	Rabbit antibody amplification
UltraWash	Selected
Nuclear counterstaining	Hematoxylin 2, 8 minutes
Post-counterstaining bluing	Bluing Reagent, 4 minutes

Table 21. *Immunohistochemistry protocol (ID 203) for E1L3N clone on Ventana Benchmark Ultra.*

Characteristics	Details
Detection kit	OptiView
Deparaffinization	72°C
Cell conditioning	ULTRA CC1, 64 minutes at 99°C
Antibody dispensation	Manual
Pre-primary peroxidase inhibition	Not selected
Primary antibody	1:100, 32 minutes at room temperature
OptiView HQ linker	12 minutes
OptiView HRP multimer	12 minutes
OptiView amplification	Not selected
Nuclear counterstaining	Hematoxylin 2, 8 minutes
Post-counterstaining bluing	Bluing Reagent, 4 minutes

Table 22. *Immunohistochemistry protocol (ID 205) for E1L3N clone on Ventana Benchmark Ultra.*

Characteristics	Details
Detection kit	OptiView
Deparaffinization	72°C
Cell conditioning	ULTRA CC1, 64 minutes at 99°C
Antibody dispensation	Manual
Pre-primary peroxidase inhibition	Selected
Primary antibody	1:100, 32 minutes at room temperature
OptiView HQ linker	12 minutes
OptiView HRP multimer	12 minutes
OptiView amplification	Not selected
Nuclear counterstaining	Hematoxylin 2, 8 minutes
Post-counterstaining bluing	Bluing Reagent, 4 minutes

Table 23. *Immunohistochemistry protocol (ID 211) for E1L3N clone on Ventana Benchmark Ultra.*

Characteristics	Details
Detection kit	OptiView
Deparaffinization	72°C
Cell conditioning	ULTRA CC1, 64 minutes at 99°C
Antibody dispensation	Manual
Pre-primary peroxidase inhibition	Selected
Primary antibody	1:100, 32 minutes at room temperature
OptiView HQ linker	12 minutes
OptiView multimer	12 minutes
OptiView amplification	Selected
H_2O_2 amplification	8 minutes
Multimer amplification	8 minutes
Nuclear counterstaining	Hematoxylin 2, 8 minutes
Post-counterstaining bluing	Bluing Reagent, 4 minutes

Table 24. *Immunohistochemistry protocol (ID 210) for E1L3N clone on Ventana Benchmark Ultra.*

Characteristics	Details
Detection kit	OptiView
Deparaffinization	72°C
Cell conditioning	ULTRA CC1 at 99°C for 64 minutes
Antibody dispensation	Manual
Pre-primary peroxidase inhibition	Selected
Primary antibody	1:100, 32 minutes at room temperature
OptiView HQ linker	8 minutes
OptiView multimer	8 minutes
OptiView amplification	Selected
H_2O_2 amplification	8 minutes
Multimer amplification	8 minutes
Nuclear counterstaining	Hematoxylin 2, 8 minutes
Post-counterstaining bluing	Bluing Reagent, 4 minutes

9.3 SUPPLEMENTARY TABLES

Table 25. *Association tests between PD-L1 concordance and measured parameters on biopsy section, to which arbitrary cutoffs were applied (a = Fisher's exact test; b = chi-square test). SP142 was assessed using the IC score, and E1L3N using the CPS.*

Biopsy-measured parameter	Parameter cutoff	PD-L1 test	p-value
Biopsies (estimate No.)	2	SP142	0.541 [a]
		E1L3N	0.073 [a]
	3	SP142	0.838 [b]
		E1L3N	0.173 [b]
	4	SP142	0.272 [b]
		E1L3N	1.000 [a]
Biopsies per cm of tumor dimension (No.)	1	SP142	0.393 [b]
		E1L3N	0.196 [b]
	1.5	SP142	0.537 [b]
		E1L3N	0.310 [a]
	2	SP142	0.729 [a]
		E1L3N	0.698 [a]
Interfaces (No.)	1	SP142	0.592 [a]
		E1L3N	0.184 [a]
	2	SP142	1.000 [a]
		E1L3N	0.081 [a]
	3	SP142	0.838 [b]
		E1L3N	0.859 [b]
	4	SP142	0.742 [a]
		E1L3N	0.492 [a]
Tumor length in biopsy (mm)	Mean	SP142	0.683 [b]
		E1L3N	0.775 [b]
	1st Quartile	SP142	0.278 [a]
		E1L3N	0.177 [a]
	Median	SP142	0.838 [b]
		E1L3N	0.501 [b]
	3rd Quartile	SP142	1.000 [a]
		E1L3N	0.310 [b]
Tumor length in biopsy per cm of tumor dimension (mm)	Mean	SP142	0.414 [b]
		E1L3N	0.987 [b]
		SP142	0.729 [a]

Biopsy-measured parameter	Parameter cutoff	PD-L1 test	p-value
	1st Quartile	E1L3N	0.665 [a]
	Median	SP142	0.414 [b]
		E1L3N	0.987 [b]
	3rd	SP142	1.000 [a]
	Quartile	E1L3N	0.727 [a]
Tumor area in biopsy (mm²)	Mean	SP142	0.152 [b]
		E1L3N	0.558 [b]
	1st	SP142	0.725 [a]
	Quartile	E1L3N	0.652 [a]
	Median	SP142	0.414 [b]
		E1L3N	0.987 [b]
	3rd	SP142	1.000 [a]
	Quartile	E1L3N	1.000 [a]
Tumor area in biopsy per cm of tumor dimension (mm²)	Mean	SP142	0.213 [a]
		E1L3N	0.633 [b]
	1st	SP142	1.000 [a]
	Quartile	E1L3N	0.659 [a]
	Median	SP142	0.153 [b]
		E1L3N	0.987 [b]
	3rd	SP142	0.725 [a]
	Quartile	E1L3N	0.456 [a]

Table 26. *Descriptive statistics stratified by IC concordance with the SP142 clone between biopsy and resection specimens (IQR: interquartile range; Min: minimum; Max: maximum).*

Parameter	IC SP142 concordance	N	Mean	SE	Median	SD	IQR	Min	Max
Biopsies (estimate No.)	true	32	2.75	0.18	3	1.02	2	1	4
	false	16	2.94	0.25	3	1.00	2	2	5
Biopsies per cm of tumor	true	32	1.70	0.24	1.38	1.34	0.96	0.31	5.71
dimension (No.)	false	16	1.29	0.23	0.97	0.92	1.01	0.42	3.33
Interfaces (No.)	true	32	2.75	0.28	3	1.59	2	0	7
	false	16	2.56	0.39	3	1.55	1.5	0	5
Interfaces per cm of tumor	true	32	1.93	0.35	1.51	1.98	1.29	0	10
dimension (No.)	false	16	1.26	0.32	0.75	1.29	1.58	0	5
Tumor length in biopsy (mm)	true	32	20.32	2.17	21.14	12.29	17.89	3.91	52.79
	false	16	22.35	2.80	20.15	11.18	15.65	9.87	44.93
Tumor length in biopsy per cm	true	32	10.96	1.27	10.68	7.21	9.85	0.70	31.37
of tumor dimension (mm)	false	16	8.74	1.25	6.50	4.99	8.58	2.51	16.77
Tumor area in biopsy (mm^2)	true	32	17.54	2.53	18.49	14.30	13.05	2.11	78.10
	false	16	15.93	2.29	12.74	9.16	13.16	5.49	36.08
Tumor area in biopsy per cm	true	32	9.68	1.37	7.77	7.73	10.71	0.76	29.83
of tumor dimension (mm^2)	false	16	6.39	1.08	4.64	4.32	5.93	1.46	14.86

Table 27. *Descriptive statistics stratified by CPS concordance with the E1L3N clone between biopsy and resection specimens (IQR: interquartile range; Min: minimum; Max: maximum).*

Parameter	CPS E1L3N concordance	N	Mean	SE	Median	SD	IQR	Min	Max
Biopsies (estimate No.)	true	31	3.00	0.16	3	0.89	2	2	5
	false	12	2.58	0.34	2	1.17	2	1	4
Biopsies per cm of neoplasia	true	31	1.80	0.25	1.5	1.38	1.46	0.31	5.71
	false	12	1.20	0.24	1.00	0.84	1.06	0.33	2.86
Interfaces (No.)	true	31	3.06	0.26	3	1.46	2	0	7
	false	12	2.42	0.47	3	1.62	2.25	0	5
Interfaces per cm of tumor	true	31	2.02	0.37	1.5	2.05	1.5	0	10
dimension (No.)	false	12	1.32	0.32	1.41	1.12	1.56	0	3.75
Tumor length in biopsy (mm)	true	31	22.24	2.19	21.96	12.19	15.58	4.53	52.79
	false	12	22.69	3.04	21.16	10.52	21.64	10.93	37.41
Tumor length in biopsy per cm	true	31	11.48	1.28	10.98	7.15	10.94	0.70	31.37
of tumor dimension (mm)	false	12	9.60	1.36	10.87	4.72	8.70	3.43	16.15
Tumor area in biopsy (mm^2)	true	31	18.72	2.53	16.73	14.08	12.17	2.56	78.10
	false	12	17.98	2.31	19.26	7.99	8.50	7.97	34.82
Tumor area in biopsy per cm of	true	31	9.91	1.36	7.31	7.59	9.84	0.76	29.83
tumor dimension (mm^2)	false	12	8.04	1.30	8.78	4.50	7.81	2.09	14.86

***Table 28**. Two-sided independent samples t-tests comparing biopsy-measured parameters between two subgroups defined by PD-L1 status concordance (concordant vs discordant) between biopsy and surgical specimens. PD-L1 was assessed using IC score for the SP142 clone and CPS for the E1L3N clone (df = degrees of freedom).*

Parameter	PD-L1 test	Student t-test	df	p-value
Biopsies (estimate No.)	SP142	-0.606	46.0	0.547
	E1L3N	1.258	41.0	0.216
Biopsies per cm of tumor dimension (No.)	SP142	1.113	46.0	0.272
	E1L3N	1.393	41.0	0.171
Interfaces (No.)	SP142	0.389	46.0	0.699
	E1L3N	1.267	41.0	0.212
Interfaces per cm of tumor dimension (No.)	SP142	1.222	46.0	0.228
	E1L3N	1.114	41.0	0.272
Tumor length in biopsy (mm)	SP142	-0.557	46.0	0.580
	E1L3N	-0.113	41.0	0.911
Tumor length in biopsy per cm of tumor dimension (mm)	SP142	1.100	46.0	0.277
	E1L3N	0.839	41.0	0.407
Tumor area in biopsy (mm^2)	SP142	0.410	46.0	0.684
	E1L3N	0.171	41.0	0.865
Tumor area in biopsy per cm of tumor dimension (mm^2)	SP142	1.578	46.0	0.121
	E1L3N	0.798	41.0	0.429

9.4 REFERENCE ATLAS

9.4.1 Predefined reference areas

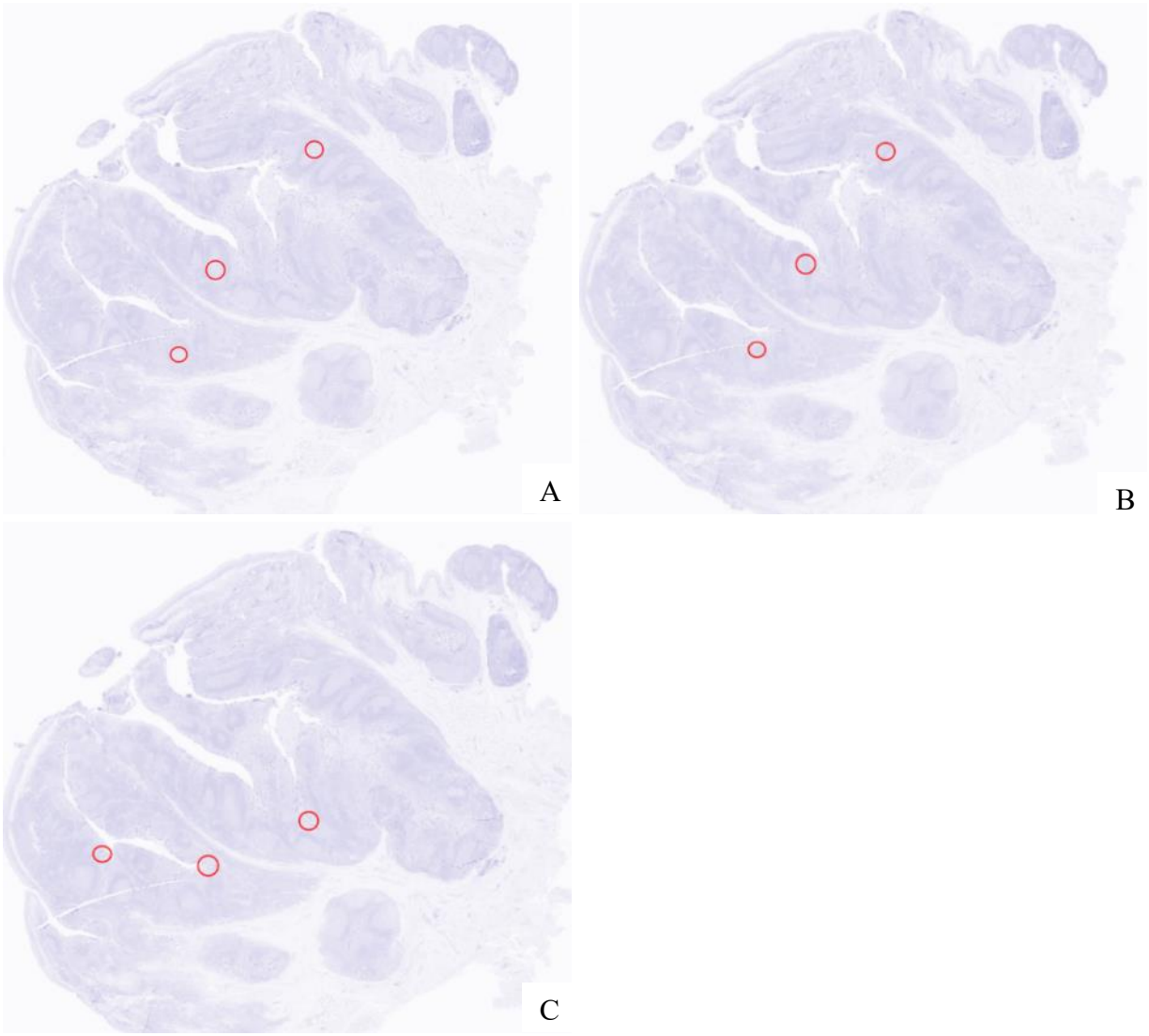

Figure 6. *Predefined reference areas within tonsil structures expected to exhibit specific PD-L1 expression (Hematoxylin). A) Germinal center; B) Mantel; C) Crypt epithelium.*

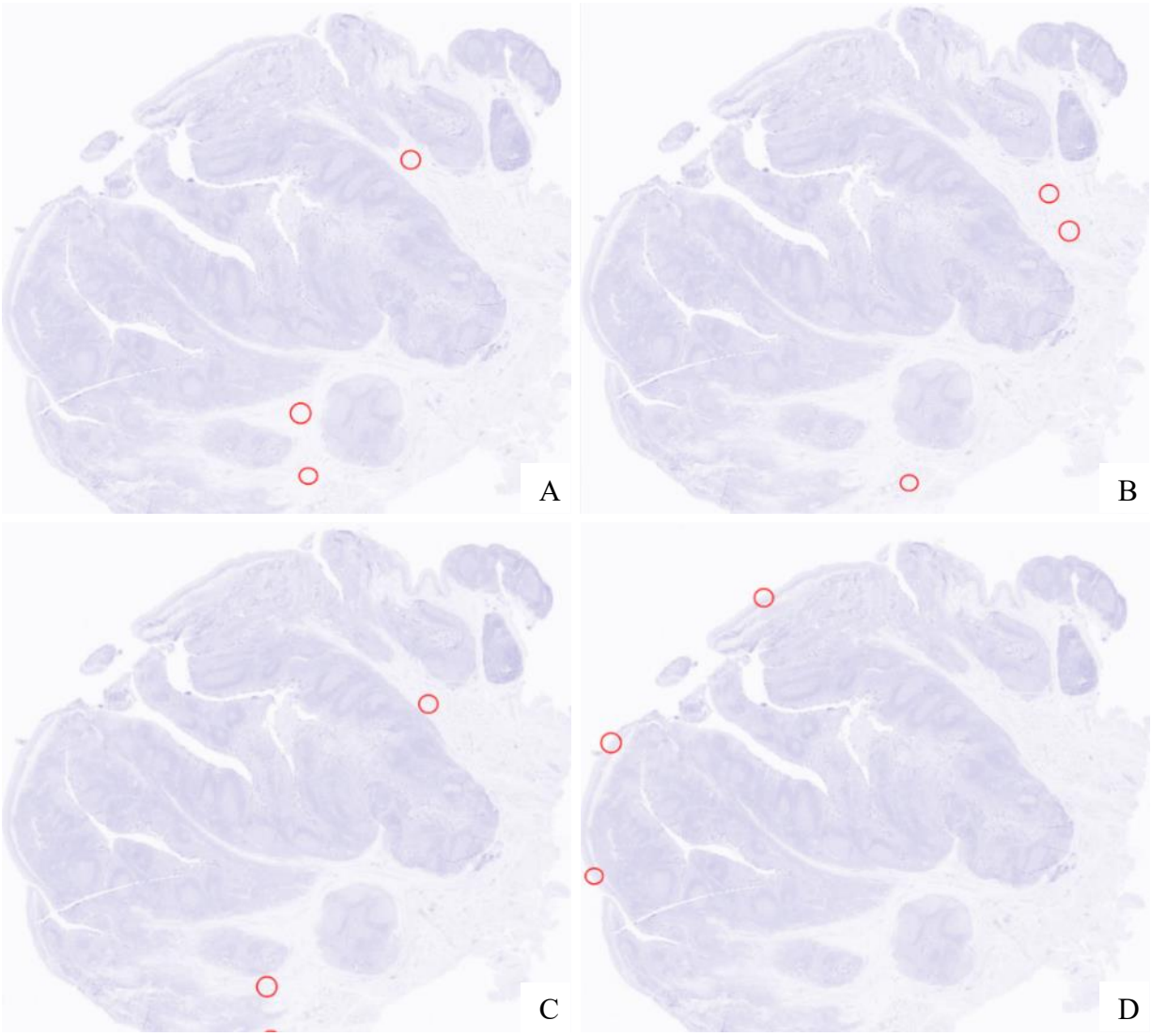

Figure 7. *Predefined reference areas within tonsil structures expected to lack PD-L1 expression (Hematoxylin). A) Intravascular erythrocytes. B) Salivary glands; C) Fibrous stroma; D) Surface epithelium.*

9.4.2 Intensity scale reference

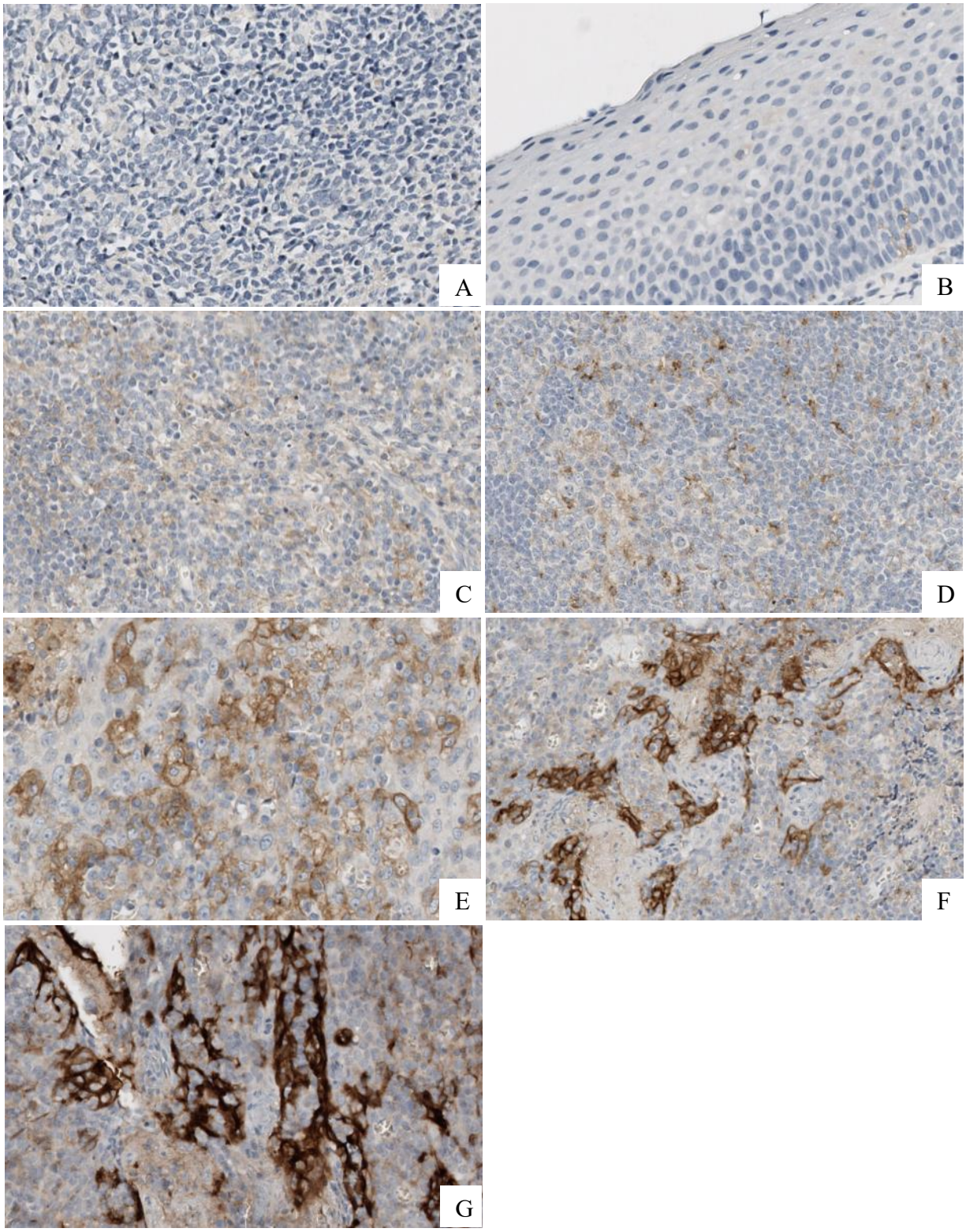

Figure 8. *Reference scale for PD-L1 immunohistochemical staining intensity, ranging from 0 (no staining) to 6 (maximum intensity). A-G) From scores 0 to score 6, respectively.*

10 ACKNOWLEDGEMENT

My deepest gratitude goes to **Dr. Enrica Bovio** for her invaluable support throughout this work, both for her technical expertise and her meticulous assistance in refining the final manuscript.

I would like to thank **Professor Renzo Luciano Boldorini** for providing access to the facilities and funding of the research laboratory he directs, and for his supervision throughout my PhD journey.

I am grateful to Roche for the kind donation of the anti-PD-L1 SP142 antibody.

Special thanks to the laboratory technicians **Alessio Ferrari** and **Carolina Cazzulino**, from the Pathology Department of the "Azienda Ospedaliero-Universitaria di Alessandria" (AOU AL), for the excellent preparation of the histological slides. I also thank the head technician, **Marzio Picollo**, and the entire technical staff for facilitating this study alongside routine clinical activities while maintaining the highest quality standards.

I wish to thank the Director of the Pathology Department, **Dr. Paola Re**, for allowing me to conduct this research within the department's facilities. My thanks also go to the collaborators of the DAIRI (Department of Integrated Research and Innovation Activities) of the AOU AL for their invaluable assistance with the administrative and bureaucratic procedures related to the clinical study; in particular, I thank **Francesca Marengo** for her extensive help.

I extend my sincere thanks to the pathologists at the satellite centers who actively participated in the study. Without their cooperation, it would not have been possible to achieve such a significant sample size given the highly selective inclusion criteria. Specifically:

- For ASL VCO: I thank the Director, **Dr. Monica Leutner**, as well as **Dr. Maurizio Muscarà**, **Dr. Maria Rosaria Bagnato**, and **Dr. Maria Cristina Pavanelli** from the Pathology Department, and **Dr. Elisabetta Garzoli** and colleagues from the Oncology Department.

- For ASL VC: I thank the Director, **Professor Guido Valente**, and **Dr. Ilenia Zanellato** from the Pathology Department, as well as the Director, **Dr. Chiara Saggia**, and colleagues from the Oncology Department.

- For AOU Novara: I once again thank the Director, **Professor Renzo Boldorini** for the opportunity to select patients at his center.

I would also like to thank the Health Managements (Direzioni Sanitarie) of the coordinating center and the three satellite centers for authorizing the study within their institutions, and data manager **Beatrice Radaelli** of the Novara Clinical Trial Center for her exceptional cooperation.

I am grateful to the reviewers of this thesis, **Professor Isabella Castellano** and **Professor Nicola Fusco**, for their time and evaluation.

Finally, I thank **Dr. Silvano Andorno** for his guidance in the final statistical analysis, and **Dr. Tiziana Altosole** (Policlinico San Martino Hospital) for her important suggestions regarding the statistical software used in this work.

11 BIBLIOGRAPHY

1. Gori, S., Miglietta, F. & Modena, A. *I Numeri Del Cancro in Italia - Mammella*. (2024).
2. Associazione Italiana di Oncologia Medica. *Linee Guida: Carcinoma Mammario Avanzato*. (2023).
3. WHO. *Breast Tumours*. vol. Volume 2 (2019).
4. Wolff, A. C. *et al.* Human epidermal growth factor receptor 2 testing in breast cancer: American society of clinical oncology/ college of American pathologists clinical practice guideline focused update. *Journal of Clinical Oncology* **36**, 2105–2122 (2018).
5. Wolff, A. C. *et al.* Human Epidermal Growth Factor Receptor 2 Testing in Breast Cancer. *Arch. Pathol. Lab. Med.* **147**, 993–1000 (2023).
6. Schettini, F. *et al.* Efficacy and safety of antibody-drug conjugates in pretreated HER2-low metastatic breast cancer: A systematic review and network meta-analysis. *Cancer Treat. Rev.* **132**, 102865 (2025).
7. Khosravi-Shahi, P., Cabezón-Gutiérrez, L. & Aparicio Salcedo, M. I. State of art of advanced triple negative breast cancer. *Breast J.* **25**, 967–970 (2019).
8. Zhang, J. *et al.* Immune-related biomarkers in triple-negative breast cancer. *Breast Cancer* **28**, 792–805 (2021).
9. Marletta, S. *et al.* Atlas of PD-L1 for Pathologists: Indications, Scores, Diagnostic Platforms and Reporting Systems. *J. Pers. Med.* **12**, 1073 (2022).
10. Geyer, F. C. *et al.* The Spectrum of Triple-Negative Breast Disease: High- and Low-Grade Lesions. *Am. J. Pathol.* **187**, 2139–2151 (2017).
11. Jiang, Y., Chen, M., Nie, H. & Yuan, Y. PD-1 and PD-L1 in cancer immunotherapy: clinical implications and future considerations. *Hum. Vaccin. Immunother.* **15**, 1111–1122 (2019).
12. Curtsinger, J. M., Johnson, C. M. & Mescher, M. F. CD8 T cell clonal expansion and development of effector function require prolonged exposure to antigen, costimulation, and signal 3 cytokine. *J. Immunol.* **171**, 5165–71 (2003).
13. Curtsinger, J. M., Lins, D. C. & Mescher, M. F. Signal 3 determines tolerance versus full activation of naive CD8 T cells: dissociating proliferation and development of effector function. *J. Exp. Med.* **197**, 1141–51 (2003).
14. Chemnitz, J. M., Parry, R. V., Nichols, K. E., June, C. H. & Riley, J. L. SHP-1 and SHP-2 associate with immunoreceptor tyrosine-based switch motif of programmed death 1

upon primary human T cell stimulation, but only receptor ligation prevents T cell activation. *J. Immunol.* **173**, 945–54 (2004).

15. Keir, M. E., Butte, M. J., Freeman, G. J. & Sharpe, A. H. PD-1 and its ligands in tolerance and immunity. *Annu. Rev. Immunol.* **26**, 677–704 (2008).
16. Mahoney, K. M., Freeman, G. J. & McDermott, D. F. The Next Immune-Checkpoint Inhibitors: PD-1/PD-L1 Blockade in Melanoma. *Clin. Ther.* **37**, 764–82 (2015).
17. Bardhan, K., Anagnostou, T. & Boussiotis, V. A. The PD1:PD-L1/2 Pathway from Discovery to Clinical Implementation. *Front. Immunol.* **7**, 550 (2016).
18. Freeman, G. J. *et al.* Engagement of the PD-1 immunoinhibitory receptor by a novel B7 family member leads to negative regulation of lymphocyte activation. *J. Exp. Med.* **192**, 1027–34 (2000).
19. Sharpe, A. H., Wherry, E. J., Ahmed, R. & Freeman, G. J. The function of programmed cell death 1 and its ligands in regulating autoimmunity and infection. *Nat. Immunol.* **8**, 239–45 (2007).
20. Sheppard, K.-A. *et al.* PD-1 inhibits T-cell receptor induced phosphorylation of the ZAP70/CD3zeta signalosome and downstream signaling to PKCtheta. *FEBS Lett.* **574**, 37–41 (2004).
21. Hui, E. *et al.* T cell costimulatory receptor CD28 is a primary target for PD-1-mediated inhibition. *Science* **355**, 1428–1433 (2017).
22. Patsoukis, N., Li, L., Sari, D., Petkova, V. & Boussiotis, V. A. PD-1 increases PTEN phosphatase activity while decreasing PTEN protein stability by inhibiting casein kinase 2. *Mol. Cell. Biol.* **33**, 3091–8 (2013).
23. Wu, T. *et al.* HMGB1 overexpression as a prognostic factor for survival in cancer: a meta-analysis and systematic review. *Oncotarget* **7**, 50417–50427 (2016).
24. Vennapusa, B. *et al.* Development of a PD-L1 Complementary Diagnostic Immunohistochemistry Assay (SP142) for Atezolizumab. *Appl. Immunohistochem. Mol. Morphol.* **27**, 92–100 (2019).
25. Erber, R. & Hartmann, A. Understanding PD-L1 Testing in Breast Cancer: A Practical Approach. *Breast Care* **15**, 481–490 (2020).
26. Ventana Medical Systems & Roche Diagnostics International. VENTANA PD-L1 (SP142) Assay Interpretation Guide for Triple-Negative Breast Carcinoma (TNBC). *https://www.rochebiomarkers.be/content/media/Files/PD-L1_SP142_interpretation_guide_TNBC.pdf* (2019).

27. Heater, N. K., Warrior, S. & Lu, J. Current and future immunotherapy for breast cancer. *J. Hematol. Oncol.* **17**, 131 (2024).
28. Debien, V. *et al.* Immunotherapy in breast cancer: an overview of current strategies and perspectives. *NPJ Breast Cancer* **9**, 7 (2023).
29. Rebaudi, F. *et al.* The landscape of combining immune checkpoint inhibitors with novel Therapies: Secret alliances against breast cancer. *Cancer Treat. Rev.* **130**, 102831 (2024).
30. European Medicines Agency. Tecentriq - Atezolizumab. https://www.ema.europa.eu/en/medicines/human/EPAR/tecentriq.
31. European Medicines Agency. Keytruda - Pembrolizumab. https://www.ema.europa.eu/en/medicines/human/EPAR/keytruda.
32. Schmid, P. *et al.* Atezolizumab and Nab-Paclitaxel in Advanced Triple-Negative Breast Cancer. *New England Journal of Medicine* **379**, 2108–2121 (2018).
33. Schmid, P. *et al.* Atezolizumab plus nab-paclitaxel as first-line treatment for unresectable, locally advanced or metastatic triple-negative breast cancer (IMpassion130): updated efficacy results from a randomised, double-blind, placebo-controlled, phase 3 trial. *Lancet Oncol.* **21**, 44–59 (2020).
34. Winer, E. P. *et al.* Pembrolizumab versus investigator-choice chemotherapy for metastatic triple-negative breast cancer (KEYNOTE-119): a randomised, open-label, phase 3 trial. *Lancet Oncol.* **22**, 499–511 (2021).
35. Nanda, R. *et al.* Pembrolizumab in patients with advanced triple-negative breast cancer: Phase Ib keynote-012 study. *Journal of Clinical Oncology* **34**, 2460–2467 (2016).
36. Adams, S. *et al.* Pembrolizumab monotherapy for previously untreated, PD-L1-positive, metastatic triple-negative breast cancer: Cohort B of the phase II KEYNOTE-086 study. *Annals of Oncology* **30**, 405–411 (2019).
37. Cortes, J. *et al.* Pembrolizumab plus Chemotherapy in Advanced Triple-Negative Breast Cancer. *New England Journal of Medicine* **387**, 217–226 (2022).
38. Associazione Italiana di Oncologia Medica. *Linee Guida: Carcinoma Mammario in Stadio Precoce*. (2023).
39. Villacampa, G. *et al.* Neoadjuvant Immune Checkpoint Inhibitors Plus Chemotherapy in Early Breast Cancer. *JAMA Oncol.* **10**, 1331 (2024).

40. Sharmni Vishnu, K., Win, T. T., Aye, S. N. & Basavaraj, A. K. Combined atezolizumab and nab-paclitaxel in the treatment of triple negative breast cancer: a meta-analysis on their efficacy and safety. *BMC Cancer* **22**, 1139 (2022).
41. Zhang, Y. *et al.* Adverse Events of PD-1 or PD-L1 Inhibitors in Triple-Negative Breast Cancer: A Systematic Review and Meta-Analysis. . **12**, 1990 (2022).
42. Elmakaty, I., Abdo, R., Elsabagh, A., Elsayed, A. & Malki, M. I. Comparative efficacy and safety of PD-1/PD-L1 inhibitors in triple negative breast cancer: a systematic review and network meta-analysis of randomized controlled trials. *Cancer Cell Int.* **23**, 90 (2023).
43. Loibl, S. *et al.* Early breast cancer: ESMO Clinical Practice Guideline for diagnosis, treatment and follow-up 5 behalf of the ESMO Guidelines Committee. *Annals of Oncology* **35**, 159–182 (2024).
44. Gennari, A. *et al.* ESMO Clinical Practice Guideline for the diagnosis, staging and treatment of patients with metastatic breast cancer ☆. *Annals of Oncology* **32**, 1475–1495 (2021).
45. Hayley Virgil. Atezolizumab TNBC Indication Withdrawn By Manufacturer After Talks With FDA. *https://www.cancernetwork.com/view/atezolizumab-tnbc-indication-withdrawn-by-manufacturer-after-talks-with-fda* (2021).
46. Ivanova, M. *et al.* PD-L1 testing in metastatic triple-negative breast cancer: Interobserver and interplatform reproducibility of CE-IVD assays for CPS and IC scores. *Hum. Pathol.* **144**, 22–27 (2024).
47. Chebib, I. & Mino-Kenudson, M. PD-L1 immunohistochemistry: Clones, cutoffs, and controversies. *APMIS* **130**, 295–313 (2022).
48. Cell Signaling. PD-L1 (E1L3N®) XP® Rabbit mAb #13684. https://www.cellsignal.com/products/primary-antibodies/pd-l1-e1l3n-xp-rabbit-mab/13684.
49. Adam, J. *et al.* Multicenter harmonization study for PD-L1 IHC testing in non-small-cell lung cancer. *Ann. Oncol.* **29**, 953–958 (2018).
50. Ahn, S. *et al.* Programmed Death Ligand 1 Immunohistochemistry in Triple-Negative Breast Cancer: Evaluation of Inter-Pathologist Concordance and Inter-Assay Variability. *J. Breast Cancer* **24**, 266–279 (2021).
51. Vlajnic, T. *et al.* PD-L1 Expression in Triple-negative Breast Cancer—a Comparative Study of 3 Different Antibodies. *Applied Immunohistochemistry & Molecular Morphology* **30**, 726–730 (2022).

52. Erick, T. K. *et al.* Concordance of PD-L1 Expression in Metastatic Triple-negative Breast Cancer Between the 22C3 and E1L3N Antibodies Using Combined Positive Scoring. *Applied Immunohistochemistry and Molecular Morphology* **32**, 417–424 (2024).
53. Song, L. *et al.* Validation of E1L3N antibody for PD-L1 detection and prediction of pembrolizumab response in non-small-cell lung cancer. *Communications Medicine* **2**, 137 (2022).
54. Parra, E. R., Villalobos, P., Mino, B. & Rodriguez-Canales, J. Comparison of Different Antibody Clones for Immunohistochemistry Detection of Programmed Cell Death Ligand 1 (PD-L1) on Non-Small Cell Lung Carcinoma. *Appl. Immunohistochem. Mol. Morphol.* **26**, 83–93 (2018).
55. Dill, E. A. *et al.* PD-L1 Expression and Intratumoral Heterogeneity Across Breast Cancer Subtypes and Stages. *American Journal of Surgical Pathology* **41**, 334–342 (2017).
56. Zdrenka, M. *et al.* Diagnostic biopsy does not accurately reflect the PD-L1 expression in triple-negative breast cancer. *Clin. Exp. Med.* **23**, 5121–5127 (2023).
57. Humphries, M. P. *et al.* Automated Tumour Recognition and Digital Pathology Scoring Unravels New Role for PD-L1 in Predicting Good Outcome in ER-/HER2+ Breast Cancer. *J. Oncol.* **2018**, 1–14 (2018).
58. Gonzalez-Ericsson, P. I. *et al.* The path to a better biomarker: application of a risk management framework for the implementation of PD-L1 and TILs as immuno-oncology biomarkers in breast cancer clinical trials and daily practice. *J. Pathol.* **250**, 667–684 (2020).
59. Humphries, M. P., Maxwell, P. & Salto-Tellez, M. QuPath: The global impact of an open source digital pathology system. *Comput. Struct. Biotechnol. J.* **19**, 852–859 (2021).
60. Bankhead, P. *et al.* QuPath: Open source software for digital pathology image analysis. *Sci. Rep.* **7**, (2017).
61. The jamovi project. Jamovi (version 2.6). https://www.jamovi.org (2025).
62. Balci, S. ClinicoPath [jamovi Module]. https://github.com/sbalci/ClinicoPathJamoviModule/ (2022).
63. Stites, E. C. & Wilen, C. B. The Interpretation of SARS-CoV-2 Diagnostic Tests. *Med* **1**, 78–89 (2020).
64. Landis, J. R. & Koch, G. G. The measurement of observer agreement for categorical data. *Biometrics* **33**, 159–74 (1977).

65. Gamer, M., Lemon, J. & Singh, I. F. Various coefficients of interrater reliabiltiy and agreement. *New York: R Package Version* (2012).

66. Marchevsky, A. M., Walts, A. E., Lissenberg-Witte, B. I. & Thunnissen, E. Pathologists should probably forget about kappa. Percent agreement, diagnostic specificity and related metrics provide more clinically applicable measures of interobserver variability. *Ann. Diagn. Pathol.* **47**, 151561 (2020).

67. Sing, T., Sander, O., Beerenwinkel, N. & Lengauer, T. ROCR: visualizing classifier performance in R. *Bioinformatics* **21**, 3940–3941 (2005).

68. Noske, A. *et al.* Comparison of assessment of programmed death-ligand 1 (PD-L1) status in triple-negative breast cancer biopsies and surgical specimens. *J. Clin. Pathol.* **77**, 239–245 (2024).

69. Dobritoiu, F. *et al.* Tissue Selection for PD-L1 Testing in Triple Negative Breast Cancer (TNBC). *Applied Immunohistochemistry & Molecular Morphology* **30**, 549–556 (2022).

70. Al-Jussani, G. N., Dabbagh, T. Z., Al-Rimawi, D. & Sughayer, M. A. Expression of PD-L1 using SP142 CDx in triple negative breast cancer. *Ann. Diagn. Pathol.* **51**, (2021).

71. Fusco, N. *et al.* Advancing the PD-L1 CPS test in metastatic TNBC: Insights from pathologists and findings from a nationwide survey. *Crit. Rev. Oncol. Hematol.* **190**, 104103 (2023).

72. Sun, W. Y., Lee, Y. K. & Koo, J. S. Expression of PD-L1 in triple-negative breast cancer based on different immunohistochemical antibodies. *J. Transl. Med.* **14**, (2016).

73. Sun, T., Zhang, H., Gao, W. & Yang, Q. The appropriate number of preoperative core needle biopsy specimens for analysis in breast cancer. *Medicine (United States)* **100**, E25400 (2021).

74. Tamaki K., K. *et al.* Comparison of core needle biopsy (CNB) and surgical specimens for accurate preoperative evaluation of ER, PgR and HER2 status of breast cancer patients. *Cancer Sci.* **101**, 2074–2079 (2010).

75. Rizzo, A. *et al. Documento di consenso: le procedure diagnostiche preoperatorie delle lesioni mammarie*. (2024).